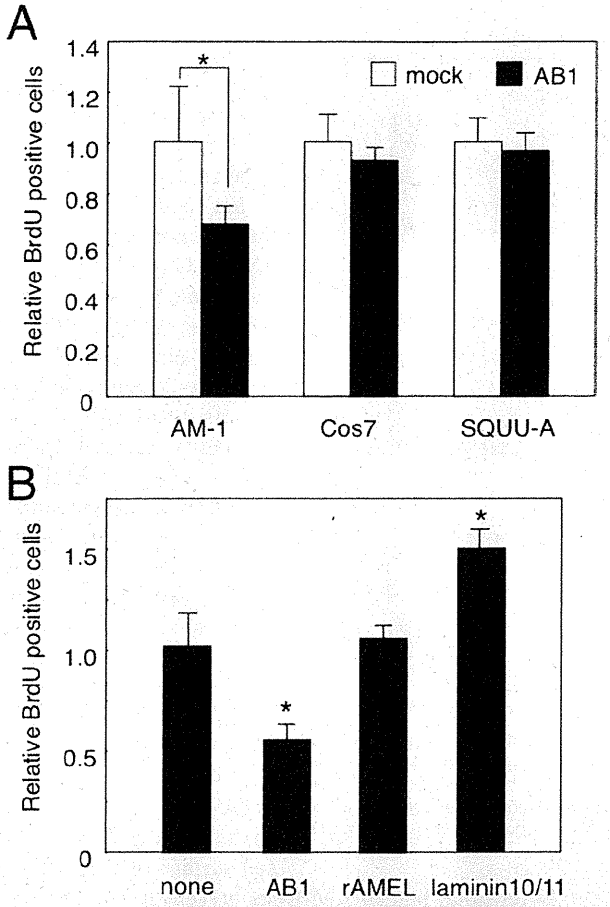

FIGURE 7. **Cell type-specific inhibition of proliferation by AMBN.** *A*, AB1. AM-1, COS-7, and SQUU-A cells were plated on dishes coated with AMBN (10 mg/ml) and cultured for 48 h. BrdUrd was incorporated into the cells for 1 h. BrdUrd-positive cells were counted. Proliferation of AM-1 cells, but not COS-7 and SQUU-A cells, was reduced on AB1 substrate. The number of BrdUrd-positive cells with mock-transfected cells was set at 100%. *B*, adhesion of AM-1 cells to dishes coated with AB1, recombinant AMEL (*rAMEL*), and laminin 10/11. The number of BrdUrd-positive cells with cells cultured on a non-coated dish was set at 100%. Statistical analysis was performed using analysis of variance (*, $p < 0.01$).

attached to the enamel matrix and the differentiation state of ameloblasts. In this paper, we identify the heparin binding domains of AMBN and demonstrate that these domains play a critical role in AMBN binding to dental epithelial cells. We also show that AMBN inhibits proliferation of human ameloblastoma cells. This inhibition is accompanied by the induction of *p21* and *p27* and *ENAM* and the reduction of *Msx2*. It was recently reported that AMBN fusion protein enhances pulpal healing and dentin formation in porcine teeth (21). In addition, AMBN promotes adhesion of periodontal ligament cells and modulates the expression of bone morphogenic protein, collagen type I, and osteocalcin (22). Those results implicate that AMBN regulates cell proliferation and differentiation through cellular signaling induced by the AMBN interaction with cells. Our finding that AMBN cell binding is mediated through the heparin binding domains suggests that AMBN interacts with heparan sulfate (HS) cell surface receptors. However, we could not detect AMBN binding to lymphoid cell lines expressing individual HS cell surface receptors, including syndecan-1, -2, and -4 (data not shown) (23). We also could not find the interaction of AMBN with glypican-1, which is expressed in ameloblasts (data not shown). Laminin is one of the heparin and integrin binding molecules. The laminin $\alpha 1$ chain LG4 module promotes cell attachment through syndecans and cell spreading through integrin $\alpha 2\beta 1$ (23). Active sequences in the LG4 of other laminin α chains have also been identified for cell attachment and heparin and syndecan binding (24–26). Further, Lys and Arg amino acid-rich regions of the LG4 module are important for heparin and HS binding. These regions may be similar to those of AMBN. A recent study (27) showed that laminin-sulfatide interaction modulates basement membrane assembly and regulates cellular signaling. It is possible that AMBN may bind cells through interacting with other co-receptors, including cell surface glycolipids and extracellular matrix.

Rodent AMBN contains a DGEA motif, which is a potential integrin-binding site of collagen I, and a thrombospondin-like cell adhesion motif, VTKG (6, 28). We found that recombinant full-length AMBN produced in mammalian cells binds specifically to primary dental epithelial cells but not to other cell types. Primary dental epithelial cells contain mixed epithelial cell populations, including inner dental epithelial cells, ameloblasts, stratum intermedium cells, and stellate cells. We found that ameloblasts, but not the other cell types, adhere to recombinant AMBN (3). In the present study, we showed that ameloblast cell lines HAT-7 and SF2 (Fig. 1) and ameloblastoma cell line AM-1 (data not shown) also bind to AMBN. The DGEA and VTKG sequences are conserved only in rodents, with little or no conservation of those motifs in other species, including human, pig, bovine, and caiman (28). Further, integrin expression disappears in differentiated ameloblasts, suggesting that other motifs in AMBN may be important for cell adhesion (18, 28, 29). The VTKG region is also known as a heparin binding domain. AMBN has positively charged Lys, Arg, and His amino acid-rich sequences in the middle and C-terminal regions (Fig. 3*A*), and KRH-rich motifs have been proposed as candidate heparin binding domains (17). The middle and C-terminal KRH-rich motifs in AMBN are conserved in human, rodent, and bovine cells, indicating that these domains may be important for cell binding. We found that full-length rat AMBN had a high affinity to heparin, whereas deletions of the heparin binding domains abrogated binding to heparin and resulted in reduced cell binding, indicating that VTKG and KRH-rich motifs serve as heparin and cell binding domains.

The EF-hand structure, which has a helix-loop-helix design, is the most common Ca^{2+}-binding motif (30). AMBN has an EF-hand motif in the C-terminal region, and proteolytic peptides from that region, particularly those migrating at 27 and 29 kDa, can be seen on SDS-PAGE assays of calcium binding. Previously, these peptides were identified in a direct ^{45}C-binding study (31) and by "Stain-all" solution, which is a detector of calcium-binding protein of enamel extract samples (32). In addition, a bioinfomatics model supports earlier experimental observations that AMBN is a bipolar,

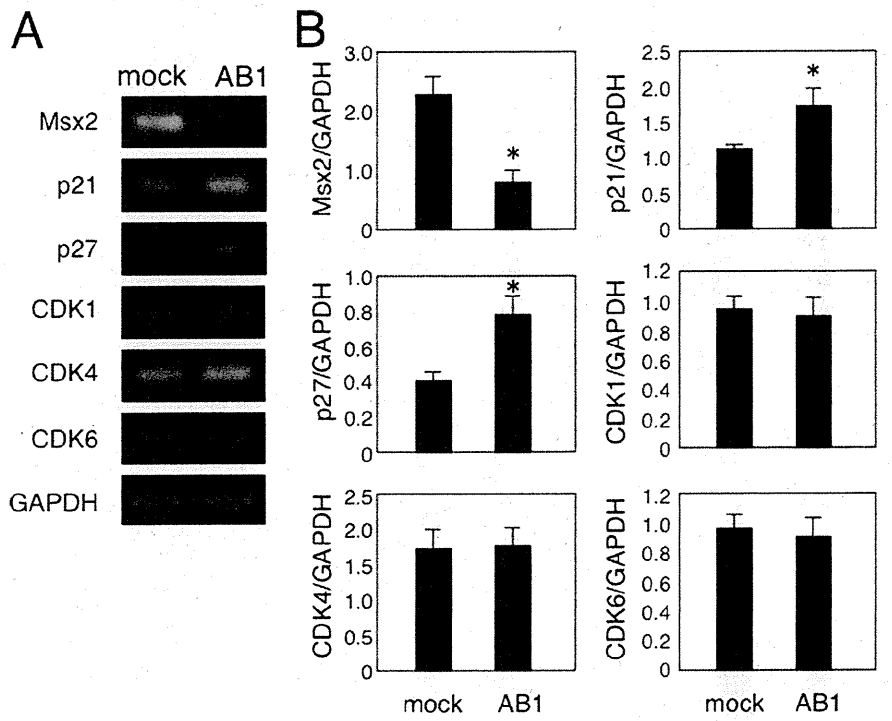

FIGURE 8. **Expression of cell cycle-regulatory genes in AMBN-overexpressing AM-1 cells.** *A*, total RNA from AM-1 cells transfected with a mock or AB1 expression vector was amplified using a semiquantitative reverse transcription-PCR method with specific primer sets. *B*, the intensity of each band was standardized with that of the glyceraldehyde-3-phosphate dehydrogenase band. *Msx2* expression was reduced, whereas expression of *p27* and *p21* was increased in AMBN-overexpressing cells. Statistical analysis was performed using analysis of variance (*, $p < 0.01$).

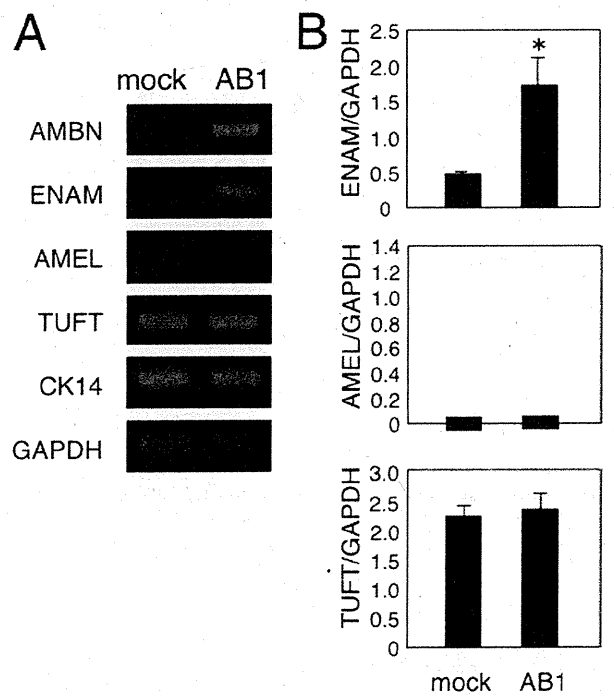

FIGURE 9. **Expression of enamel matrix proteins in AMBN-overexpressing AM-1 cells.** *A*, total RNA from AM-1 cells transfected with a mock or AB1 expression vector was amplified using a semiquantitative reverse transcription-PCR method with specific primer sets for tooth-specific genes. *B*, the intensity of the *AMBN*, *AMEL*, and *TUFT* bands was standardized with that of the glyceraldehyde-3-phosphate dehydrogenase band. *ENAM*, but not *AMEL*, was induced by AMBN overexpression. Statistical analysis was performed using analysis of variance (*, $p < 0.01$).

two-domain protein that interacts with Ca^{2+} ions. The primary structure of AMBN can be divided into two chemically and physically distinct regions: a basic N-terminal region and acidic C-terminal region. It has been speculated that the three-dimensional structure of AMBN is dramatically changed in water and in the presence of Ca^{2+} ions after molecular dynamics stimulation and energy optimization (19). Our findings agree with these reports, since AMBN heparin binding ability changed dramatically in the presence of EDTA, and this change was dependent on the EF-hand motif (Fig. 4, *C* and *D*). However, attachment of dental epithelium to AMBN did not increase in the presence of EDTA (Fig. 2), suggesting that other calcium-dependent molecules may be involved in cell binding. Further, in amelogenesis, AMBN is cleaved after secretion by several protease, including MMP-20 (33). The cleaved C-terminal half of AMBN is located near the cell surface of ameloblasts, and the N-terminal half of AMBN is present in the calcified front of enamel (34), indicating that the C-terminal region of AMBN may be important for cell binding *in vivo*. Recently, *AMBN* has been reported to appear in three different molecular sizes (37, 55, and 66 kDa) in both ameloblasts and enamel matrix during postnatal development (35). There may be various transcripts of *Ambn* that are developmentally expressed and interact with AMEL (16). Interestingly, 37-kDa AMBN containing three heparin binding domains is expressed in the early stage of ameloblast differentiation. These results indicate that the C-terminal region of AMBN is important for cell adhesion, ameloblast differentiation, and enamel nucleation.

Amelogenin and AMBN were shown to be expressed in not only ameloblasts but also odontoblasts (36). The surface of dentin has a layer of keratan sulfate rich in sulfated sialic acids and GlcNAc emanating from the dentinal tubules, which is a potent ligand for amelogenin (16). Ameloblastin may have a similar function with dentin matrix and odontoblast differentiation. Additional experiments are needed to resolve this issue.

Epithelial odontogenic tumors are histologically related to the remnants of odontogenic epithelium, which includes the dental lamina, enamel organ, and Hertwig's epithelial root sheath (37). Actively growing dental lamina is present within the jaws for a considerable time after birth, and because of the widespread presence of odontogenic epithelium, some tumors may arise from residues of those cells. AMBN is expressed by differentiated ameloblasts and also in forming Hertwig's epithelial root sheath cells and can be used as a marker of their migration (38). Previous immunohistochem-

ical studies have attempted to investigate the differentiation of neoplastic cells in odontogenic tumors; however, it was reported that AMBN, AMEL, and ENAM were not expressed in ameloblastoma cells (39, 40). *Ambn*-null mice develop odontogenic tumors of dental epithelium origin in addition to severe enamel hypoplasia. Further, because the ameloblasts disappear after eruption, tooth enamel is never replaced or repaired, and odontogenic epithelium almost completely disappears when tooth formation is completed in those mice. However, it is known that discrete clusters of odontogenic epithelial cells remain in the periodontal ligament as the epithelial cell rests of Malassez (ERM) (41). Although the function of ERM cells is still unclear, it is considered that a number of odontogenic tumors arise from them (41, 42). Recently, it was reported that ERM cells express AMBN but not AMEL or ENAM (43). It was also reported that *AMBN* gene mutations are associated with odontogenic tumors, including ameloblastomas (12, 44). In the study, we showed that AM-1 cells do not express AMBN, but overexpression of AMBN suppresses proliferation of AM-1 cells. Taken together, we speculate that AMBN functions as an odontogenic tumor suppressor.

Msx2, a homeobox-containing transcription factor, was previously shown to be expressed in undifferentiated ameloblasts, whereas it is down-regulated in differentiated ameloblasts (20). In *Ambn*-null ameloblasts, an abnormal up-regulation of Msx2 was observed (3), suggesting that AMBN inhibits the expression of Msx2 in normal tooth development. Our finding that AMBN transfection dramatically reduced Msx2 expression supports the notion that AMBN negatively regulates Msx2 expression. It has been suggested that Msx homeobox genes inhibit differentiation through up-regulation of cyclin D1 (45). In AMBN-transfected AM-1 cells, the cyclin-dependent kinase inhibitors *p21* and *p27* were up-regulated, whereas the expressions of *CDK1*, *-4*, and *-6* were not changed. Thus, down-regulation of *Msx2* and up-regulation of *p21* and *p27* by AMBN expression probably cause reduced proliferation of AM-1 cells. Further, the overexpression of AMBN lacking three heparin binding domains did not inhibit proliferation of AM-1 cells, suggesting the crucial role of the heparin binding domains of AMBN for the inhibition of AM-1 proliferation. It is conceivable that AMBN induces cellular signaling for these cellular changes by its interaction with AM-1 cells.

REFERENCES

1. Damsky, C. H., and Werb, Z. (1992) *Curr. Opin. Cell Biol.* **4,** 772–781
2. Arikawa-Hirasawa, E., Wilcox, W. R., Le, A. H., Silverman, N., Govindraj, P., Hassell, J. R., and Yamada, Y. (2001) *Nat. Genet.* **27,** 431–434
3. Fukumoto, S., Kiba, T., Hall, B., Iehara, N., Nakamura, T., Longenecker, G., Krebsbach, P. H., Nanci, A., Kulkarni, A. B., and Yamada, Y. (2004) *J. Cell Biol.* **167,** 973–983
4. Krebsbach, P. H., Lee, S. K., Matsuki, Y., Kozak, C. A., Yamada, K. M., and Yamada, Y. (1996) *J. Biol. Chem.* **271,** 4431–4435
5. Fong, C. D., Slaby, I., and Hammarström, L. (1996) *J. Bone Miner. Res.* **11,** 892–898
6. Cerný, R., Slaby, I., Hammarström, L., and Wurtz, T. (1996) *J. Bone Miner. Res.* **11,** 883–891
7. Paine, M. L., Wang, H. J., Luo, W., Krebsbach, P. H., and Snead, M. L. (2003) *J. Biol. Chem.* **278,** 19447–19452
8. MacDougall, M., Simmons, D., Gu, T. T., Forsman-Semb, K., Mårdh, C. K., Mesbah, M., Forest, N., Krebsbach, P. H., Yamada, Y., and Berdal, A. (2000) *Eur. J. Oral Sci.* **108,** 303–310
9. Nakamura, Y., Slaby, I., Spahr, A., Pezeshki, G., Matsumoto, K., and Lyngstadaas, S. P. (2006) *Calcif. Tissue Int.* **78,** 278–284
10. Ramadas, K., Jose, C. C., Subhashini, J., Chandi, S. M., and Viswanathan, F. R. (1990) *Cancer* **66,** 1475–1479
11. Newman, L., Howells, G. L., Coghlan, K. M., DiBiase, A., and Williams, D. M. (1995) *Br. J. Oral Maxillofac. Surg.* **33,** 47–50
12. Perdigão, P. F., Gomez, R. S., Pimenta, F. J., and De Marco, L. (2004) *Oral Oncol.* **40,** 841–846
13. Yuasa, K., Fukumoto, S., Kamasaki, Y., Yamada, A., Fukumoto, E., Kanaoka, K., Saito, K., Harada, H., Arikawa-Hirasawa, E., Miyagoe-Suzuki, Y., Takeda, S., Okamoto, K., Kato, Y., and Fujiwara, T. (2004) *J. Biol. Chem.* **279,** 10286–10292
14. de Vega, S., Iwamoto, T., Nakamura, T., Hozumi, K., McKnight, D. A., Fisher, L. W., Fukumoto, S., and Yamada, Y. (2007) *J. Biol. Chem.* **282,** 30878–30888
15. Nishiguchi, M., Yuasa, K., Saito, K., Fukumoto, E., Yamada, A., Hasegawa, T., Yoshizaki, K., Kamasaki, Y., Nonaka, K., Fujiwara, T., and Fukumoto, S. (2007) *Arch. Oral Biol.* **52,** 237–243
16. Ravindranath, H. H., Chen, L. S., Zeichner-David, M., Ishima, R., and Ravindranath, R. M. (2004) *Biochem. Biophys. Res. Commun.* **323,** 1075–1083
17. Yamada, Y., and Kleinman, H. K. (1992) *Curr. Opin. Cell Biol.* **4,** 819–823
18. Fukumoto, S., Miner, J. H., Ida, H., Fukumoto, E., Yuasa, K., Miyazaki, H., Hoffman, M. P., and Yamada, Y. (2006) *J. Biol. Chem.* **281,** 5008–5016
19. Vymetal, J., Slabý, I., Spahr, A., Vondrásek, J., and Lyngstadaas, S. P. (2008) *Eur. J. Oral Sci.* **116,** 124–134
20. Maas, R., and Bei, M. (1997) *Crit. Rev. Oral Biol. Med.* **8,** 4–39
21. Nakamura, Y., Slaby, I., Spahr, A., Pezeshki, G., Matsumoto, K., and Lyngstadaas, S. P. (2006) *Calcif. Tissue Int.* **78,** 278–284
22. Zeichner-David, M., Chen, L. S., Hsu, Z., Reyna, J., Caton, J., and Bringas, P. (2006) *Eur. J. Oral Sci.* **114,** Suppl. 1, 244–253; discussion 254–246, 381–242
23. Hozumi, K., Suzuki, N., Nielsen, P. K., Nomizu, M., and Yamada, Y. (2006) *J. Biol. Chem.* **281,** 32929–32940
24. Hoffman, M. P., Engbring, J. A., Nielsen, P. K., Vargas, J., Steinberg, Z., Karmand, A. J., Nomizu, M., Yamada, Y., and Kleinman, H. K. (2001) *J. Biol. Chem.* **276,** 22077–22085
25. Utani, A., Nomizu, M., Matsuura, H., Kato, K., Kobayashi, T., Takeda, U., Aota, S., Nielsen, P. K., and Shinkai, H. (2001) *J. Biol. Chem.* **276,** 28779–28788
26. Okazaki, I., Suzuki, N., Nishi, N., Utani, A., Matsuura, H., Shinkai, H., Yamashita, H., Kitagawa, Y., and Nomizu, M. (2002) *J. Biol. Chem.* **277,** 37070–37078
27. Li, S., Liquari, P., McKee, K. K., Harrison, D., Patel, R., Lee, S., and Yurchenco, P. D. (2005) *J. Cell Biol.* **169,** 179–189
28. Fukumoto, S., Yamada, A., Nonaka, K., and Yamada, Y. (2005) *Cells Tissues Organs* **181,** 189–195
29. Fukumoto, S., and Yamada, Y. (2005) *Connect. Tissue Res.* **46,** 220–226
30. Kobayashi, C., and Takada, S. (2006) *Biophys. J.* **90,** 3043–3051
31. Fukae, M., and Tanabe, T. (1987) *Adv. Dent. Res.* **1,** 261–266
32. Yamakoshi, Y., Tanabe, T., Oida, S., Hu, C. C., Simmer, J. P., and Fukae, M. (2001) *Arch. Oral Biol.* **46,** 1005–1014
33. Iwata, T., Yamakoshi, Y., Hu, J. C., Ishikawa, I., Bartlett, J. D., Krebsbach, P. H., and Simmer, J. P. (2007) *J. Dent. Res.* **86,** 153–157
34. Nanci, A., Zalzal, S., Lavoie, P., Kunikata, M., Chen, W., Krebsbach, P. H., Yamada, Y., Hammarström, L., Simmer, J. P., Fincham, A. G., Snead, M. L., and Smith, C. E. (1998) *J. Histochem. Cytochem.* **46,** 911–934
35. Ravindranath, R. M., Devarajan, A., and Uchida, T. (2007) *J. Biol. Chem.* **282,** 36370–36376
36. Nagano, T., Oida, S., Ando, H., Gomi, K., Arai, T., and Fukae, M. (2003) *J. Dent. Res.* **82,** 982–986
37. Melrose, R. J. (1999) *Semin. Diagn. Pathol.* **16,** 271–287
38. Zeichner-David, M., Oishi, K., Su, Z., Zakartchenko, V., Chen, L. S., Arzate, H., and Bringas, P., Jr. (2003) *Dev. Dyn.* **228,** 651–663
39. Saku, T., Okabe, H., and Shimokawa, H. (1992) *J. Oral Pathol. Med.* **21,**

113–119
40. Takata, T., Zhao, M., Uchida, T., Kudo, Y., Sato, S., and Nikai, H. (2000) *Virchows Arch.* **436,** 324–329
41. Rincon, J. C., Young, W. G., and Bartold, P. M. (2006) *J. Periodontal Res.* **41,** 245–252
42. Goldblatt, L. I., Brannon, R. B., and Ellis, G. L. (1982) *Oral Surg. Oral Med. Oral Pathol.* **54,** 187–196
43. Shinmura, Y., Tsuchiya, S., Hata, K., and Honda, M. J. (2008) *J. Cell Physiol.* **217,** 728–738
44. Toyosawa, S., Fujiwara, T., Ooshima, T., Shintani, S., Sato, A., Ogawa, Y., Sobue, S., and Ijuhin, N. (2000) *Gene* **256,** 1–11
45. Hu, G., Lee, H., Price, S. M., Shen, M. M., and Abate-Shen, C. (2001) *Development* **128,** 2373–2384
46. Aumailley, M., Bruckner-Tuderman, L., Carter, W. G., Deutzmann, R., Edgar, D., Ekblom, P., Engel, J., Engvall, E., Hohenester, E., Jones, J. C., Kleinman, H. K., Marinkovich, M. P., Martin, G. R., Mayer, U., Meneguzzi, G., Miner, J. H., Miyazaki, K., Patarroyo, M., Paulsson, M., Quaranta, V., Sanes, J. R., Sasaki, T., Sekiguchi, K., Sorokin, L. M., Talts, J. F., Tryggvason, K., Uitto, J., Virtanen, I., von der Mark, K., Wewer, U. M., Yamada, Y., and Yurchenco, P. D. (2005) *Matrix Biol.* **24,** 326–332

RESEARCH REPORTS
Biological

J. Hatakeyama[1], S. Fukumoto[2], T. Nakamura[2], N. Haruyama[1], S. Suzuki[1], Y. Hatakeyama[3], L. Shum[3], C. W. Gibson[4], Y. Yamada[2], and A. B. Kulkarni[1]*

[1]Functional Genomics Section and [2]Molecular Biology Section, Laboratory of Cell and Developmental Biology, National Institute of Dental and Craniofacial Research, and [3]Cartilage Biology and Orthopedics Branch, National Institute of Arthritis and Musculoskeletal and Skin Diseases, National Institutes of Health, 30 Convent Dr., MSC 4395, Bethesda, MD 20892, USA; and [4]Department of Anatomy and Cell Biology, University of Pennsylvania School of Dental Medicine, Philadelphia, PA 19104, USA; *corresponding author, ak40m@nih.gov

J Dent Res 88(4):318-322, 2009

Synergistic Roles of Amelogenin and Ameloblastin

ABSTRACT

Amelogenin and ameloblastin, the major enamel matrix proteins, are important for enamel mineralization. To identify their synergistic roles in enamel development, we generated *Amel X*$^{-/-}$*/Ambn*$^{-/-}$ mice. These mice showed additional enamel defects in comparison with *Amel X*$^{-/-}$ or *Ambn*$^{-/-}$ mice. In 7-day-old *Amel X*$^{-/-}$*/Ambn*$^{-/-}$ mice, not only was the ameloblast layer irregular and detached from the enamel surface, as in *Ambn*$^{-/-}$, but also, the enamel width was significantly reduced in the double-null mice as compared with *Amel X*$^{-/-}$ or *Ambn*$^{-/-}$ mice. Proteomic analysis of the double-null teeth revealed increased levels of RhoGDI (Arhgdia), a Rho-family-specific guanine nucleotide dissociation inhibitor, which is involved in important cellular processes, such as cell attachment. Both *Amel X*$^{-/-}$*/Ambn*$^{-/-}$ mice and *Ambn*$^{-/-}$ mice displayed positive staining with RhoGDI antibody in the irregularly shaped ameloblasts detached from the matrix. Ameloblastin-regulated expression of RhoGDI suggests that Rho-mediated signaling pathway might play a role in enamel formation.

KEY WORDS: enamel, amelogenin, ameloblastin, knockout mice, RhoGDI (Arhgdia).

DOI: 10.1177/0022034509334749

Received August 25, 2008; Last revision January 8, 2009; Accepted January 12, 2009

A supplemental appendix to this article is published electronically only at http://jdr.sagepub.com/supplemental.

INTRODUCTION

Dental enamel is the most highly mineralized tissue in the body, and is formed as a result of mineralization of enamel matrices secreted by ameloblasts. Ameloblasts secrete several enamel matrix proteins, such as amelogenins, ameloblastin, and enamelin. These enamel matrix proteins are processed and degraded by proteases such as MMP20 and KLK4 during enamel mineralization (Bartlett *et al.*, 1996; Simmer *et al.*, 1998). The highly orchestrated secretion of enamel matrix proteins and their proper degradation are critical for normal enamel formation.

The amelogenin proteins are highly conserved across species, and constitute 90% of the enamel organic matrix. Based on the results from our study of *Amel X*$^{-/-}$ mice, amelogenins play an important role in enamel biomineralization (Gibson *et al.*, 2001; Hatakeyama *et al.*, 2003). In the *Amel X*$^{-/-}$ mice, ameloblast differentiation was relatively normal, but an abnormally thin enamel layer was formed (Gibson *et al.*, 2001, 2005).

It was concluded that amelogenins are essential for well-organized hydroxyapatite prism formation and elongation during enamel development, and for producing normal enamel thickness, but not for the initiation of enamel formation. Our recent studies on transgenic mice, which express the most abundant amelogenin form, M180, in the amelogenin null background, demonstrated that M180 could significantly rescue the enamel defects of the amelogenin null mice (Li *et al.*, 2008). Self-assembly of amelogenin proteins into nanospheres has been recognized as a key factor in controlling the orientation and elongated growth of crystals during the mineralizing process in enamel (Du *et al.*, 2005). Transgenic mice that express an amelogenin protein with a mutation either at the N or C terminus showed that the N-terminal domain of amelogenin might be involved in the formation of nanospheres (Paine *et al.*, 2003a), whereas the C-terminal region could contribute to stability and homogeneity in sizes of nanospheres, preventing mineral crystal fusion to form larger structures prematurely (Moradian-Oldak and Goldberg, 2005; Moradian-Oldak *et al.*, 2006). In addition, we have recently reported amelogenin's function for osteoclast differentiation in periodontal ligament tissue (Hatakeyama *et al.*, 2006).

Ameloblastin, also known as amelin or sheathlin, is an enamel-specific glycoprotein, which is the most abundant non-amelogenin enamel matrix protein (Cerný *et al.*, 1996; Krebsbach *et al.*, 1996; Fong *et al.*, 1998), and serves as a cell adhesion molecule for ameloblasts, but not for dental epithelial cells (Fukumoto *et al.*, 2004, 2005). Ameloblastin expression in ameloblasts peaks at the secretory stage and diminishes at the maturation stage. Transgenic mice overexpressing ameloblastin in ameloblasts have impaired enamel structures, suggesting the importance of normal levels of ameloblastin in enamel formation (Paine *et al.*, 2003b). Furthermore, in *Ambn*$^{-/-}$ mice, the dental epithelium differentiates into enamel-secreting ameloblasts, but the cells detach from the

matrix surface at the secretory stage and lose polarity. In ameloblasts of *Ambn*$^{-/-}$ teeth, the expression of amelogenins is reduced to about 20% of that of *Ambn*$^{+/+}$ teeth, while other enamel matrix proteins are expressed at nearly normal levels (Fukumoto *et al.*, 2004). These results suggested that ameloblastin is essential in maintaining normal ameloblast differentiation and attachment to the enamel matrix. Thus, the cellular functions of amelogenin and ameloblastin are apparently distinct, and in this paper we report potential synergistic functions of these 2 enamel proteins.

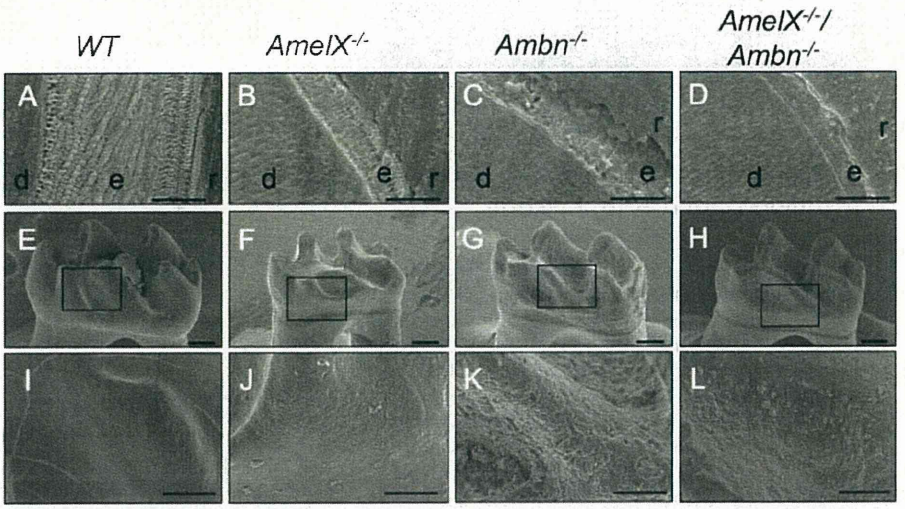

Figure 1. Scanning electron microscopy analysis of teeth from *Amel X*$^{-/-}$, *Ambn*$^{-/-}$, *Amel X*$^{-/-}$/*Ambn*$^{-/-}$, and wild-type mice. **(A-D)** Incisors from the 6-week-old mutant and wild-type mice; the enamel (e) in junction with dentin (d) is shown. Note the thin aprismatic structure in *Amel X*$^{-/-}$ mice **(B).** The enamel width of *Amel X*$^{-/-}$/*Ambn*$^{-/-}$ **(D)** mice markedly reduced as compared with that of the *Ambn*$^{-/-}$ mice **(C). (E-L)** Molars of the 6-week-old wild-type and mutant mice; note the small crown size of *Amel X*$^{-/-}$ mice **(F)** and the double-mutant **(H).** The enamel from *Amel X*$^{-/-}$(F), *Ambn*$^{-/-}$ **(G)**, and *Amel X*$^{-/-}$/*Ambn*$^{-/-}$ **(H)** appeared abnormal as compared with that in the wild-type mice (E). **(I-L)** Teeth from all 3 mutant mice mimic the amelogenesis imperfecta phenotype. *Amel X*$^{-/-}$/*Ambn*$^{-/-}$ enamel appeared less cobbled as compared with *Ambn*$^{-/-}$ enamel. Bars in A-D = 50 μm; bars in E-L = 250 μm. e, enamel; d, dentin; r, resin.

MATERIALS & METHODS

Amel X$^{-/-}$/*Ambn*$^{-/-}$ Mice

Targeted disruption of amelogenin (*Amel X*) and ameloblastin (*Ambn*) genes has been described previously (Gibson *et al.*, 2001; Fukumoto *et al.*, 2004). *Amel X*$^{-/-}$ mice were mated with *Ambn*$^{-/-}$ mice to generate double-heterozygous mice, which were interbred to generate *Amel X*$^{-/-}$/*Ambn*$^{-/-}$ mice. (Detailed information on generation and genotyping is described in the online Appendix and Appendix Fig. 1.) Mutant mice were initially analyzed in a C57BL/6 × 129/SvEv mixed genetic background and later in an enriched C57BL/6 background by being back-crossed 4 x with C57BL/6 mice. Standard NIH guidelines were followed for housing, feeding, and breeding the mice. These studies were carried out with the approval of the NIDCR Animal Care and Use Committee.

Scanning Electron Microscopic (SEM) Analyses of Incisors and Molars

Incisors and molars from wild-type and mutant mice were coated with gold and photographed by scanning electron microscopy at 20 kV (Jeol JSM T330A, Jeol, Inc., Peabody, MA, USA), and energy-dispersive spectroscopy (Kevex X-ray, Scotts Valley, CA, USA).

To observe the enamel crystals, we embedded the specimens in epoxy resin, cut them with an ISOMET low-speed saw (Buehler, Lake Bluff, IL, USA), treated them with 40% phosphoric acid for 10 sec and 10% sodium hypochlorite for 30 sec, and then coated them with gold.

Preparation of Tissue Sections and Immunohistochemistry

Post-natal (P) days 1 (P1) and 7 (P7) mouse skulls were dissected and fixed with 4% paraformaldehyde in phosphate-buffered saline (PBS) for 16 hrs at 4°C. Tissues were decalcified with 250 mM EDTA/PBS and embedded in paraffin for paraffin sections or in OCT compound (Sakura Finetechnical Co., Torrance, CA, USA) for frozen sectioning. Frozen sections were cut at 8-μm intervals on a cryostat (2800 Frigocut, Leica Inc., Wetzlar, Germany). Paraffin sections were cut at 5-μm intervals on a microtome (RM2155, Leica Inc.). For detailed morphological analysis, sections were stained with hematoxylin and eosin Y (Sigma, St. Louis, MO, USA). Frozen sections were immunostained for RhoGDI with goat polyclonal antibodies against mouse RhoGDI (Santa Cruz Biotechnology, Santa Cruz, CA, USA) overnight at 4°C at a dilution of 1:100. After being washed with PBS, the sections were incubated with peroxidase-conjugated mouse antibodies against goat IgG (Vector Laboratories, Burlingame, CA, USA), treated with diaminobenzidine substrate, and counterstained with hematoxylin for light microscopy. For control, frozen sections were incubated with secondary antibody only.

RESULTS

Defective Enamel Formation in *Amel X*$^{-/-}$/*Ambn*$^{-/-}$ Mice

SEM analysis of incisors revealed hypoplastic enamel and a lack of prism pattern in *Amel X*$^{-/-}$, *Ambn*$^{-/-}$, and *Amel X*$^{-/-}$/*Ambn*$^{-/-}$ mice that is the hallmark of organized mineral crystals in normal enamel (Figs. 1A-1D). Enamel width was much thinner in *Amel X*$^{-/-}$/*Ambn*$^{-/-}$ mice as compared with that in *Amel X*$^{-/-}$ and *Ambn*$^{-/-}$ mice. As in *Ambn*$^{-/-}$ mice, flat plate-like structures extended perpendicularly from the enamel surface to the dentin enamel junction in *Amel X*$^{-/-}$/*Ambn*$^{-/-}$ mice (Figs. 1C, 1D). The enamel surfaces appeared cobbled in both *Amel X*$^{-/-}$ (Fig. 1J) and *Ambn*$^{-/-}$ (Fig. 1K) mice. However, in *Amel X*$^{-/-}$/*Ambn*$^{-/-}$ mice, the molar surfaces appeared less cobbled than in *Amel X*$^{-/-}$ and *Ambn*$^{-/-}$ mice (Fig. 1L). Elemental

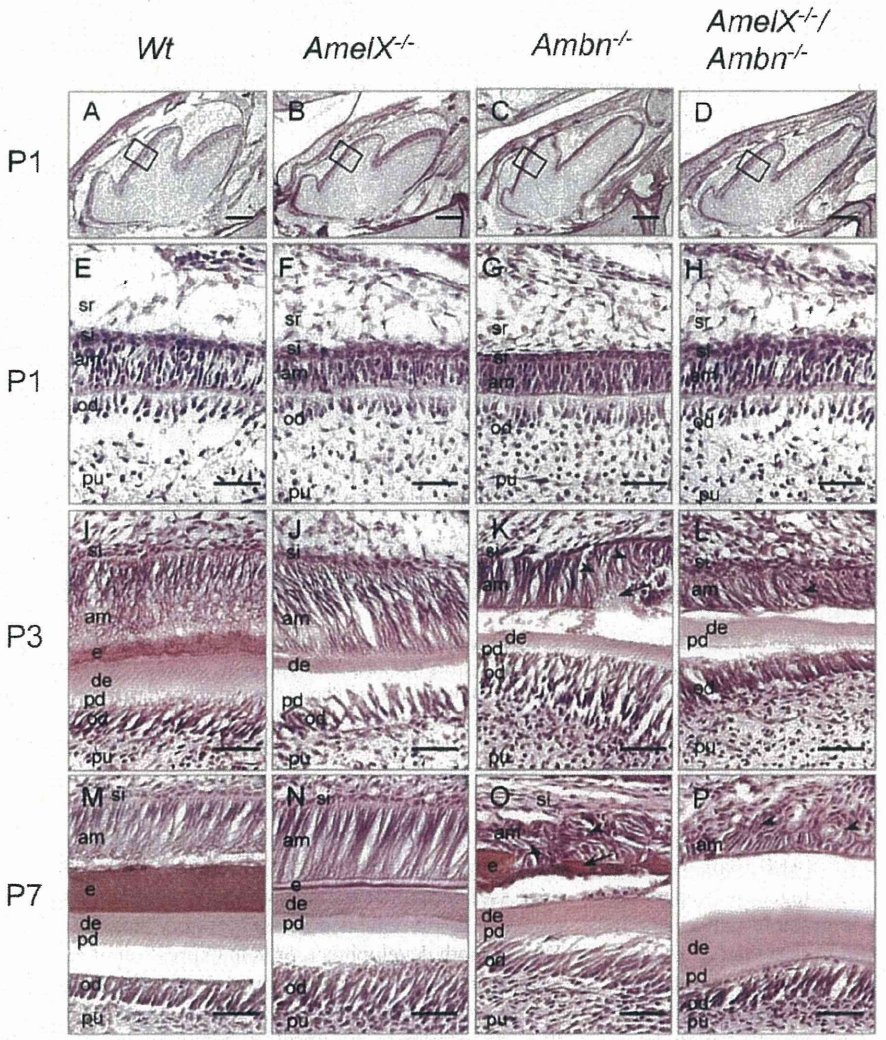

Figure 2. Histological analysis of teeth from the wild-type, *Amel X*$^{-/-}$, *Ambn*$^{-/-}$, and *Amel X*$^{-/-}$/*Ambn*$^{-/-}$ mice. Hematoxylin-eosin staining of the sagittal sections of the mandibular first molars of P1 **(A-H)**, P3 **(I-L)**, and P7 **(M-P)** wild-type and mutant mice: wild-type **(A,E,I,M)**, *Amel X*$^{-/-}$ **(B,F,J,N)**, *Ambn*$^{-/-}$ **(C,G,K,O)**, and *Amel X*$^{-/-}$/*Ambn*$^{-/-}$ mice **(D,H,L,P)**. P3 and P7 *Ambn*$^{-/-}$ ameloblasts display multiple layers containing abnormal calcified structures (Figs. 2K and 2O, arrows). *Amel X*$^{-/-}$/*Ambn*$^{-/-}$ ameloblasts also form multiple layers; however, they do not contain the calcified structures (Figs. 2L and 2P, arrowhead). am, ameloblast; si, stratum intermedium; e, enamel; pd, predentin; de, dentin; od, odontoblast; pu, pulp; sr, stellate reticulum. Bars in A-D = 500 μm; bars in E-P = 50 μm.

analysis indicated that the composition was similar to that of hydroxyapatite, indicating a normal formation of mineral in the absence of the amelogenin and ameloblastin proteins. The Ca/P molar ratio was also not significantly different in the teeth of all null mice and the WT controls (almost 1.5; data not shown).

Unlike Ambn$^{-/-}$ Ameloblasts, *Amel X*$^{-/-}$/*Ambn*$^{-/-}$ Ameloblasts Do Not Develop Calcified Nodules

In early stages of molar development up to P1, no differences were observed in either shape or size of the tooth buds of WT, *Amel X*$^{-/-}$, *Ambn*$^{-/-}$, and *Amel X*$^{-/-}$/*Ambn*$^{-/-}$ mice (Figs. 2A-2D). At P1, dentin formation of molars had begun, and dental epithelium had started to elongate and polarize with the apical nuclear localization in all of these mice (Figs. 2E-2H). Thus, cellular organization of ameloblasts and odontoblasts was similar in these mice at the pre-secretory stage. However, at P3, ameloblasts of *Ambn*$^{-/-}$ and *Amel X*$^{-/-}$/*Ambn*$^{-/-}$ mice started to detach from the matrix layer and lost the cell polarity with the centralized nuclear localization (Figs. 2K, 2L), whereas normal ameloblasts were polarized, elongated, and formed an enamel matrix in WT and *Amel X*$^{-/-}$ mice (Figs. 2I, 2J). At P7, *Ambn*$^{-/-}$ and *Amel X*$^{-/-}$/*Ambn*$^{-/-}$ ameloblasts completely lost their polarity (short and round) and accumulated to form a multilayered structure (Figs. 2O, 2P, arrowhead), in contrast to the single layer of WT and *Amel X*$^{-/-}$ ameloblasts (Figs. 2M, 2N). Interestingly, *Ambn*$^{-/-}$ ameloblasts contained calcified nodules (Fig. 2O, arrow), but *Amel X*$^{-/-}$/*Ambn*$^{-/-}$ cells did not (Fig. 2P).

Increased RhoGDI Expression in *Amel X*$^{-/-}$/*Ambn*$^{-/-}$ Ameloblasts

We utilized proteomic analysis to identify 24-kDa-size protein, which was increased in *Amel X*$^{-/-}$/*Ambn*$^{-/-}$ ameloblasts (Appendix Fig. 2). Using MALDI analysis, we identified this protein as RhoGDI. For further analysis of RhoGDI expression patterns in developing mouse molars, we carried out immunohistochemical analysis. At P1, weak RhoGDI expression was observed in ameloblasts and odontoblasts of the WT, *Amel X*$^{-/-}$, *Ambn*$^{-/-}$, and *Amel X*$^{-/-}$/*Ambn*$^{-/-}$ mice (Figs. 3A-3D). However, at P7, the ameloblasts of WT and *Amel X*$^{-/-}$ mice had no noticeable RhoGDI expression (Figs. 3E, 3F), whereas irregularly shaped ameloblasts in *Ambn*$^{-/-}$ and *Amel X*$^{-/-}$/*Ambn*$^{-/-}$ mice showed sustained expression of RhoGDI (Figs. 3G, 3H). Calcified nodules were also detected adjacent to the irregular ameloblast layer in *Ambn*$^{-/-}$ mice (Fig. 3G, arrow), but not in *Amel X*$^{-/-}$/*Ambn*$^{-/-}$ mice. We also noted increased expression of RhoGDI in the lower first molars of the 7-day-old *Amel X*$^{-/-}$/*Ambn*$^{-/-}$ mice by RT-PCR (Appendix Fig. 3).

DISCUSSION

To delineate potential synergistic roles of amelogenins and ameloblastin, we analyzed teeth from the wild-type, *Amel X*$^{-/-}$,

Ambn$^{-/-}$, and *Amel X*$^{-/-}$/*Ambn*$^{-/-}$ mice. Our analysis revealed that the *Amel X*$^{-/-}$/*Ambn*$^{-/-}$ mice displayed additional enamel defects. As compared with the *Amel X*$^{-/-}$ and *Ambn*$^{-/-}$ mice, enamel width was markedly reduced in *Amel X*$^{-/-}$/ *Ambn*$^{-/-}$ mice. Although ameloblast morphology was similar in *Ambn*$^{-/-}$ and *Amel X*$^{-/-}$/ *Ambn*$^{-/-}$ mice, calcified nodules observed in *Ambn*$^{-/-}$ ameloblasts were absent in the double-null ameloblasts. These additional defects in *Amel X*$^{-/-}$/*Ambn*$^{-/-}$ ameloblasts suggest a possible synergism in the cellular functions of amelogenins and ameloblastin.

Surprisingly, *Amel X*$^{-/-}$/*Ambn*$^{-/-}$ mice still showed a very thin layer of enamel, in spite of the lack of the 2 most abundant ECM proteins secreted by ameloblasts to form normal enamel. We found that enamelin was still expressed in the *Amel X*$^{-/-}$/*Ambn*$^{-/-}$ teeth (based on our RT-PCR analysis; data not shown). The enamelin gene (ENAM) has also been implicated in human amelogenesis imperfecta (Kim *et al.*, 2005). *Enam*$^{-/-}$ mice did not form normal enamel, because of the lack of mineralization at the secretory surfaces of the ameloblasts (Hu *et al.*, 2008). In addition, ENAM point mutation resulted in the phenotype resembling amelogenesis imperfecta (Masuya *et al.*, 2005). Therefore, it is possible that enamelin might be involved in enamel formation in the *Amel X*$^{-/-}$/*Ambn*$^{-/-}$ mice. In addition to enamelin, other ECM proteins might play a role in enamel formation in these mice, and their identification will require further studies. We had previously reported that amelogenins are involved in osteoclast differentiation in PDL cells, and furthermore, one can speculate that its lack in the double-null mice might contribute in some way to the formation of thinner enamel. Interestingly, SEM analysis of molars and incisors indicated smoother enamel in the *Amel X*$^{-/-}$/*Ambn*$^{-/-}$ mice as compared with *Ambn*$^{-/-}$ enamel. This phenotypic difference can be possibly attributed to the presence of irregular calcified nodules in *Ambn*$^{-/-}$ ameloblasts, and one can speculate that these nodules are formed because of the residual amelogenin in these mice (Fukumoto *et al.*, 2004).

Our proteomic studies identified an increased protein level of RhoGDI (Arhgdia) in *Amel X*$^{-/-}$/*Ambn*$^{-/-}$ teeth. RhoGDI, a Rho-family-specific guanine nucleotide dissociation inhibitor, forms a tight complex with Rho GTPases and inactivates Rho GTPases function as a cytosolic molecule. Reduced expression or inactivation of RhoGDIs releases Rho GTPases from the complex and translocates Rho GTPases into the membrane for activation of Rho signaling pathways (Takai *et al.*, 1995). Rho GTPases such as Rho, Rac, and Cdc42 are known to regulate assembly of filamentous actin (F-actin) and the organization of the actin cytoskeleton, and the regulation of gene transcription, cell cycle, microtubule dynamics, vesicle transport, and numerous enzymatic activities. In the wild-type teeth, RhoGDI was expressed in undifferentiated dental epithelium, but its expression was down-regulated in the secretory stage of ameloblasts. During tooth development, protein expression of RhoGDI is not altered at the early stage in *Amel X*$^{-/-}$, *Ambn*$^{-/-}$, and *Amel X*$^{-/-}$/ *Ambn*$^{-/-}$ ameloblasts. However, in later stages, when cells continue to proliferate and form multicellular layers in *Amel X*$^{-/-}$/ *Ambn*$^{-/-}$ mice, RhoGDI expression is increased. The Rho signaling pathways in murine ameloblasts are known to induce F-actin product (Li *et al.*, 2005). F-actin-rich regions have been described, and these include Tomes' process, distal terminal webs, and distal ends of ruffled or smooth-ended ameloblasts in rat incisors (Nishikawa and Kitamura, 1986).

Interestingly, the human *Amel X* gene has been shown to reside in a "nested" gene structure within intron 1 of the *ARHGAP6* gene that encodes Rho GAP, which regulates RhoA activity (Hall and Nobes, 2000; Prakash *et al.*, 2005). In some cases, expression of nested and host genes is simultaneously up- and down-regulated by common regulatory elements (Peters and Ross, 2001). It is possible that the expression of *Amel X* and *ARHGAP6* genes might be similarly regulated. Rho is recognized as a molecular switch (Hall and Nobes, 2000), which normally cycles from the active GTP-bound form to the inactive GDP-bound form (Li *et al.*, 2005), thereby regulating downstream events leading to changes in the cytoskeleton. It has been shown that Rac1 and Cdc42, downstream of Rho signaling, are regulators of cell spreading and formation of lamellipodia and filopodia (Clark *et al.*, 1998; Hall, 1998), and cell polarization

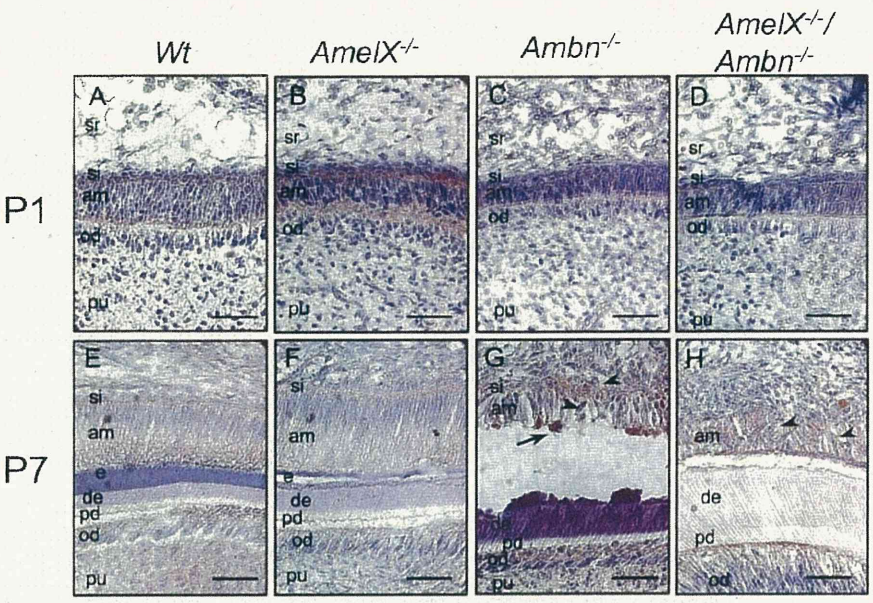

Figure 3. RhoGDI expression in the ameloblasts of the wild-type, *Amel X*$^{-/-}$, *Ambn*$^{-/-}$, and *Amel X*$^{-/-}$/ *Ambn*$^{-/-}$ mice. Sagittal sections of the incisors from the wild-type **(A,E)**, *Amel X*$^{-/-}$ **(B,F)**, *Ambn*$^{-/-}$ **(C,G)**, and *Amel X*$^{-/-}$/*Ambn*$^{-/-}$ mice **(D,H)** were stained with the RhoGDI antibody as described in MATERIALS & METHODS. Note positive staining in the detached ameloblasts of *Ambn*$^{-/-}$ **(C,G)** and *Amel X*$^{-/-}$/ *Ambn*$^{-/-}$ mice **(D,H)**. Bars = 50 μm. am, ameloblast; od, odontoblast; pu, pulp; si, stratum intermedium; e, enamel; d, dentin; pd, predentin.

(Etienne-Manneville and Hall, 2002; Cau and Hall, 2005). Rac1 and Cdc42 regulate laminin-10/11-mediated cell spreading and filopodia formation of the dental epithelium (Fukumoto *et al.*, 2006). Increased expression of RhoGDI in *Amel* $X^{-/-}$/*Ambn*$^{-/-}$ teeth might inhibit active Rho GTP, resulting in irregular ameloblast morphology.

In summary, our study suggests that the enamel matrix proteins such as amelogenins and ameloblastin are not only required for the formation of a proper matrix for well-orchestrated enamel biomineralization, but also have synergistic cellular functions during enamel development.

ACKNOWLEDGMENTS

We thank Drs. Aya Yamada and Yoko Kamasaki for generous help with SEM analysis, and Harry Grant for editorial assistance. This work was supported by the Division of Intramural Research of the National Institute of Dental and Craniofacial Research.

REFERENCES

Bartlett JD, Simmer JP, Xue J, Margolis HC, Moreno EC (1996). Molecular cloning and mRNA tissue distribution of a novel matrix metalloproteinase isolated from porcine enamel organ. *Gene* 183:123-128.

Cau J, Hall A (2005). Cdc42 controls the polarity of the actin and microtubule cytoskeletons through two distinct signal transduction pathways. *J Cell Sci* 118(Pt 12):2579-2587.

Cerný R, Slaby I, Hammarström L, Wurtz T (1996). A novel gene expressed in rat ameloblasts codes for proteins with cell binding domains. *J Bone Miner Res* 11:883-891.

Clark EA, King WG, Brugge JS, Symons M, Hynes RO (1998). Integrin-mediated signals regulated by members of the rho family of GTPases. *J Cell Biol* 142:573-586.

Du C, Falini G, Fermani S, Abbott C, Moradian-Oldak J (2005). Supramolecular assembly of amelogenin nanospheres into birefringent microribbons. *Science* 307:1450-1454; *erratum* in *Science* 309:2166, 2005.

Etienne-Manneville S, Hall A (2002). Rho GTPases in cell biology. *Nature* 420:629-635.

Fong CD, Cerný R, Hammarström L, Slaby I (1998). Sequential expression of an amelin gene in mesenchymal and epithelial cells during odontogenesis in rats. *Eur J Oral Sci* 106(Suppl 1):324-330.

Fukumoto S, Kiba T, Hall B, Iehara N, Nakamura T, Longenecker G, *et al.* (2004). Ameloblastin is a cell adhesion molecule required for maintaining the differentiation state of ameloblasts. *J Cell Biol* 167:973-983.

Fukumoto S, Yamada A, Nonaka K, Yamada Y (2005). Essential roles of ameloblastin in maintaining ameloblast differentiation and enamel formation. *Cells Tissues Organs* 181:189-195.

Fukumoto S, Miner JH, Ida H, Fukumoto E, Yuasa K, Miyazaki H, *et al.* (2006). Laminin alpha5 is required for dental epithelium growth and polarity and the development of tooth bud and shape. *J Biol Chem* 281:5008-5016.

Gibson CW, Yuan ZA, Hall B, Longenecker G, Chen E, Thyagarajan T, *et al.* (2001). Amelogenin-deficient mice display an amelogenesis imperfecta phenotype. *J Biol Chem* 276:31871-31875.

Gibson CW, Kulkarni AB, Wright JT (2005). The use of animal models to explore amelogenin variants in amelogenesis imperfecta. *Cells Tissues Organs* 181:196-201.

Hall A (1998). Rho GTPases and the actin cytoskeleton. *Science* 279: 509-514.

Hall A, Nobes CD (2000). Rho GTPases: molecular switches that control the organization and dynamics of the actin cytoskeleton. *Philos Trans R Soc Lond B Biol Sci* 355:965-970.

Hatakeyama J, Sreenath T, Hatakeyama Y, Thyagarajan T, Shum L, Gibson CW, *et al.* (2003). The receptor activator of nuclear factor-kappa B ligand-mediated osteoclastogenic pathway is elevated in amelogenin-null mice. *J Biol Chem* 278:35743-35748.

Hatakeyama J, Philp D, Hatakeyama Y, Haruyama N, Shum L, Aragon MA, *et al.* (2006). Amelogenin-mediated regulation of osteoclastogenesis and periodontal cell proliferation and igration. *J Dent Res* 85: 144-149.

Hu JCC, Hu Y, Smith CE, McKee MD, Wright JT, Yamakoshi Y, *et al.* (2008). Enamel defects and ameloblast-specific expression in *Enam* knock-out/*lacZ* knock-in mice. *J Biol Chem* 283:10858-10871.

Kim JW, Seymen F, Lin BP, Kiziltan B, Gencay K, Simmer JP, *et al.* (2005). ENAM mutations in autosomal-dominant amelogenesis imperfecta. *J Dent Res* 84:278-282.

Krebsbach PH, Lee SK, Matsuki Y, Kozak CA, Yamada KM, Yamada Y (1996). Full-length sequence, localization, and chromosomal mapping of ameloblastin. A novel tooth-specific gene. *J Biol Chem* 271:4431-4435.

Li Y, Decker S, Yuan ZA, DenBesten PK, Aragon MA, Jordan-Sciutto K, *et al.* (2005). Effects of sodium fluoride on the actin cytoskeleton of murine ameloblasts. *Arch Oral Biol* 50:681-688.

Li Y, Suggs C, Wright JT, Yuan Z, Aragon M, Fong H, *et al.* (2008). Partial rescue of the amelogenin null dental enamel phenotype. *J Biol Chem* 283:15056-15062.

Masuya H, Shimizu K, Sezutsu H, Sakuraba Y, Nagano J, Shimizu A, *et al.* (2005). Enamelin (Enam) is essential for amelogenesis: ENU-induced mouse mutants as models for different clinical subtypes of human amelogenesis imperfecta (AI). *Hum Mol Genet* 14:575-583.

Moradian-Oldak J, Goldberg M (2005). Amelogenin supra-molecular assembly in vitro compared with the architecture of the forming enamel matrix. *Cells Tissues Organs* 181:202-218.

Moradian-Oldak J, Du C, Falini G (2006). On the formation of amelogenin microribbons. *Eur J Oral Sci* 114(Suppl 1):289-296.

Nishikawa S, Kitamura H (1986). Localization of actin during differentiation of the ameloblast, its related epithelial cells and odontoblasts in the rat incisor using NBD-phallacidin. *Differentiation* 30:237-243.

Paine ML, Luo W, Zhu DH, Bringas P Jr, Snead ML (2003a). Functional domains for amelogenin revealed by compound genetic defects. *J Bone Miner Res* 18:466-472.

Paine ML, Wang HJ, Luo W, Krebsbach PH, Snead ML (2003b). A transgenic animal model resembling amelogenesis imperfecta related to ameloblastin overexpression. *J Biol Chem* 278:19447-19452.

Peters MF, Ross CA (2001). Isolation of a 40-kDa Huntingtin-associated protein. *J Biol Chem* 276:3188-3194.

Prakash SK, Gibson CW, Wright JT, Boyd C, Cormier T, Sierra R, *et al.* (2005). Tooth enamel defects in mice with a deletion at the Arhgap 6/Amel X locus. *Calcif Tissue Int* 77:23-29.

Simmer JP, Fukae M, Tanabe T, Yamakoshi Y, Uchida T, Xue J, *et al.* (1998). Purification, characterization, and cloning of enamel matrix serine proteinase 1. *J Dent Res* 77:377-386.

Takai Y, Sasaki T, Tanaka K, Nakanishi H (1995). Rho as a regulator of the cytoskeleton. *Trends Biochem Sci* 20:227-231.

Published June 20, 2011

THE JOURNAL OF CELL BIOLOGY

Pannexin 3 functions as an ER Ca^{2+} channel, hemichannel, and gap junction to promote osteoblast differentiation

Masaki Ishikawa,[1] Tsutomu Iwamoto,[1,2] Takashi Nakamura,[1,2] Andrew Doyle,[1] Satoshi Fukumoto,[2] and Yoshihiko Yamada[1]

[1]Laboratory of Cell and Developmental Biology, National Institute of Dental and Craniofacial Research, National Institutes of Health, Bethesda, MD 20892
[2]Department of Pediatric Dentistry, Tohoku University Graduate School of Dentistry, Sendai 980-8576, Japan

The pannexin proteins represent a new gap junction family. However, the cellular functions of pannexins remain largely unknown. Here, we demonstrate that pannexin 3 (Panx3) promotes differentiation of osteoblasts and ex vivo growth of metatarsals. Panx3 expression was induced during osteogenic differentiation of C2C12 cells and primary calvarial cells, and suppression of this endogenous expression inhibited differentiation. Panx3 functioned as a unique Ca^{2+} channel in the endoplasmic reticulum (ER), which was activated by purinergic receptor/phosphoinositide 3-kinase (PI3K)/Akt signaling, followed by activation of calmodulin signaling for differentiation. Panx3 also formed hemichannels that allowed release of ATP into the extracellular space and activation of purinergic receptors with the subsequent activation of PI3K–Akt signaling. Panx3 also formed gap junctions and propagated Ca^{2+} waves between cells. Blocking the Panx3 Ca^{2+} channel and gap junction activities inhibited osteoblast differentiation. Thus, Panx3 appears to be a new regulator that promotes osteoblast differentiation by functioning as an ER Ca^{2+} channel and a hemichannel, and by forming gap junctions.

Introduction

Gap junctions mediate intracellular signaling events, which in turn regulate various downstream cellular and physiological functions (Bennett and Verselis, 1992; Scemes et al., 2007). Gap junction proteins allow ions and small molecules to pass between adjacent cells via gap junctions, and between cells and the extracellular space via hemichannels (Unger et al., 1999; Bruzzone et al., 2001). In vertebrates, gap junction proteins are categorized into two families, connexins (Cxs) and pannexins (Panxs; Vinken et al., 2006). The connexin family has >20 members and has been relatively well characterized. Dysregulation and mutations of connexins cause several human diseases, including cancer, hypertension, atherosclerosis, and developmental abnormalities (Laird, 2006). The pannexin family is less well known and consists of only three members: Panx1, -2, and -3 (Panchin et al., 2000; Baranova et al., 2004; D'hondt et al., 2009).

Correspondence to Yoshihiko Yamada: yoshi.yamada@nih.gov

Abbreviations used in this paper: ALP, alkaline phosphatase; CA, constitutively active; CaM, calmodulin; CaMKII, CaM kinase II; CBX, carbenoxolone; CN, calcineurin; DN, dominant negative; IP3R, inositol trisphosphate 3 receptor; Ocn, osteocalcin; PI3K, phosphoinositide 3-kinase; PLC, phospholipase C; PPADS, pyridoxal-phosphate-6-azophenyl-2′,4′-disulfonate; RyR, ryanodine receptor; SERCA, sarco/endoplasmic reticulum Ca^{2+}-ATPase.

Panx1 is ubiquitously expressed, especially in the central nervous system. Panx2 is also expressed in the central nervous system (Bruzzone et al., 2003). Panx3 is expressed in skin, cochlea, and in developing hard tissues including cartilage and bone (Penuela et al., 2007; Penuela et al., 2008; Wang et al., 2009; Iwamoto et al., 2010). Panx3 is induced in the prehypertrophic zone in developing growth plates, and it inhibits parathyroid hormone–mediated chondrocyte proliferation through its hemichannel activity and promotes differentiation in culture (Iwamoto et al., 2010). Panx3 expression is also known to inhibit proliferation of keratinocytes (Celetti et al., 2010), although the underlying mechanism has not yet been established.

Ca^{2+} is a universal intracellular signaling molecule that regulates cell proliferation, differentiation, morphology, and function (Berridge et al., 2000b). Intracellular Ca^{2+} concentration ($[Ca^{2+}]_i$) can rise more than fivefold via Ca^{2+} influx from the extracellular space and/or release from the ER, an intracellular Ca^{2+} storage

Supplemental Material can be found at:
http://jcb.rupress.org/content/suppl/2011/06/20/jcb.201101050.DC1.html
Original image data can be found at:
http://jcb-dataviewer.rupress.org/jcb/browse/4054

The Rockefeller University Press $30.00
J. Cell Biol. Vol. 193 No. 7 1257–1274
www.jcb.org/cgi/doi/10.1083/jcb.201101050

Published June 20, 2011

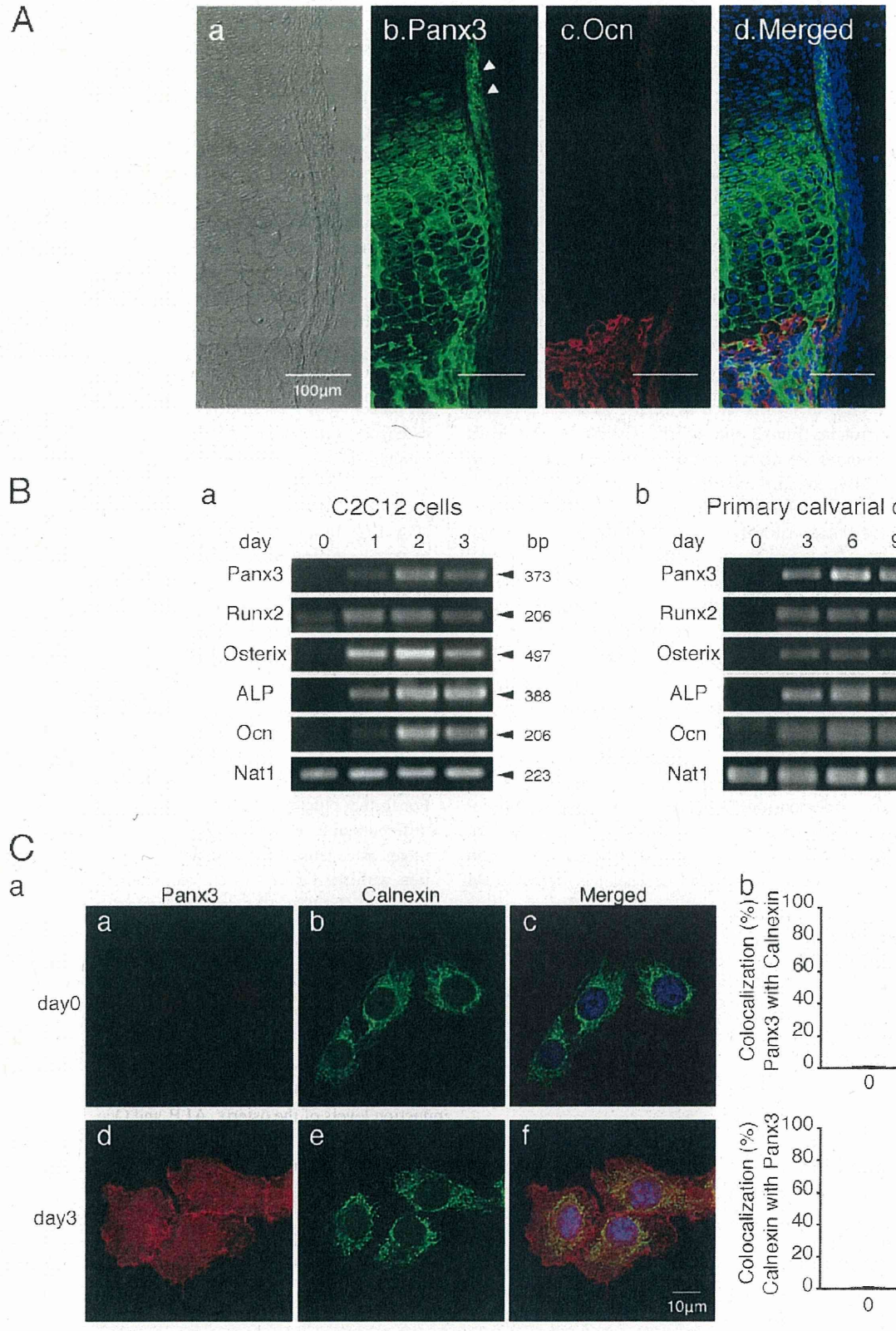

Figure 1. **Expression of Panx3 in growth plates, C2C12 cells, and primary calvarial cells.** (A) Immunostaining of newborn mouse growth plates. Image under light microscopy (a), Panx3 (b), Ocn (c), Hoechst nuclear staining (blue), and merged image (d). Arrowheads, perichondrium/periosteum. (B) Semi-quantitative RT-PCR. C2C12 cells (a) and primary calvarial cells (b) were cultured with BMP2 and ascorbate, respectively, at day 0. Panx3 was induced

Published June 20, 2011

organelle, when cells are activated by extracellular stimuli. Inositol trisphosphate 3 (IP3) receptors (IP3Rs) are ubiquitously expressed and act as ER Ca^{2+} channels upon IP3 binding (Mikoshiba, 2007). IP3 synthesis for activation of IP3R ER channels can be induced by many stimuli. For example, external ATP can bind purinergic receptors (P2Rs) in the plasma membrane, and this triggers activation of phospholipase C (PLC) and subsequent IP3 generation. Ryanodine receptors (RyRs) are also known to function as ER Ca^{2+} channels in some tissues (Fill and Copello, 2002). More recently, Panx1 was unexpectedly found to function as an ER Ca^{2+} channel in prostate cancer cells (Vanden Abeele et al., 2006).

The Ca^{2+} binding protein calmodulin (CaM) is one of the major Ca^{2+} signaling mediators (Berridge et al., 2000b), and the CaM pathway regulates osteoblast differentiation (Zayzafoon, 2006). Osteoblasts differentiate from mesenchymal stem cells and form bone through endochondral and intramembranous ossification. Growth factors such as BMP2 induce the master osteogenic proteins Runx2 and osterix (Osx/Sp7). This leads to the activation of osteogenic marker genes, and subsequently, to terminal differentiation of osteoblasts (Fujita et al., 2004; Mukherjee and Rotwein, 2009). Many signaling molecules have been identified that positively or negatively regulate osteoblast differentiation. For example, phosphoinositide 3-kinase (PI3K)/Akt signaling is crucial for osteoblast differentiation (Fujita et al., 2004; Mukherjee and Rotwein, 2009), whereas p53 is a negative regulator for osteogenesis (Wang et al., 2006). In the case of CaM, binding to Ca^{2+} activates downstream signaling molecules such as CaM kinase II (CaMKII) and calcineurin (CN), and promotes osteoblast differentiation (Zayzafoon et al., 2005).

Our previous study showed that Panx3 mRNA is expressed in osteoprogenitors and osteoblasts, and prompted us to explore in more detail the role of Panx3 in osteoblast differentiation. In the present study, we demonstrate that Panx3 is induced during osteoblast differentiation and promotes differentiation. We found that Panx3 functions as an ER Ca^{2+} channel and is regulated through a PI3K–Akt pathway. The Panx3 Ca^{2+} ER channels regulate CaM pathways and promote osteogenic differentiation. Panx3, acting as a hemichannel, also promotes the release of ATP into the extracellular space. The released ATP may bind to P2Rs followed by activation of PI3K–Akt signaling. Furthermore, Panx3 gap junctions propagate a Ca^{2+} wave between cells and enhance osteoblast differentiation. Our results reveal that Panx3 plays a multifunctional role as a new regulator of osteoblast differentiation.

Results

Panx3 expression and localization in growth plates and differentiating osteoblasts

We previously reported that Panx3 mRNA is expressed in prehypertrophic chondrocytes, in the perichondrium/periosteum, and in osteoblasts in the growth plate (Iwamoto et al., 2010). Immunohistochemistry showed that the Panx3 protein was expressed in prehypertrophic and hypertrophic chondrocytes, as well as in the perichondrium/periosteum, which are progenitors for osteoblasts (arrowheads in Fig. 1 A, b). Immunostaining of osteocalcin (Ocn), an osteoblast marker, showed a distinct boundary between cartilage and bone. Panx3 was also expressed in osteoblasts (Fig. 1 A, c and d).

To study the role of Panx3 in osteoblast differentiation, we analyzed the expression of Panx3 mRNA in the osteoprogenitor cell line C2C12, and in primary calvarial cells from newborn mice (Fig. 1 B). Panx3 mRNA was not detectable in undifferentiated cells. However, when the cells differentiated into osteoblasts, Panx3 expression was found concomitantly with the induction of osteoblast marker genes such as Runx2, osterix, alkaline phosphatase (ALP), and Ocn (Fig. 1 B, a and b). Similar induction of Panx3 mRNA expression was observed during osteogenic differentiation of MC3T3-E1 and C3H10T1/2 cells (unpublished data).

We next examined subcellular localization of the Panx3 protein in C2C12 cells using fluorescence confocal microscopy (Fig. 1 C). In differentiating C2C12 cells, Panx3 was localized to the plasma membrane and within cell–cell contact areas, as well as diffusely in the cytosol. Calnexin, an ER marker, was colocalized with Panx3, which suggests that Panx3 is localized in the ER (Fig. 1 C, f). Quantitative analysis revealed that 60% of the Panx3 protein was colocalized with calnexin, whereas 90% of calnexin was colocalized with Panx3 (Fig. 1 C, b). These results suggest that Panx3 may function at multiple subcellular regions.

Panx3 promotes osteoblast differentiation

For further elucidation of the Panx3 function during osteoblast differentiation, we examined whether Panx3 expression promotes osteogenic differentiation of C2C12 cells. After transfection with the Panx3 expression vector (pEF1/Panx3; Fig. S1, A and B), C2C12 cells were induced to differentiate, and mRNA expression of osteoblast marker genes was analyzed over time using real-time quantitative PCR (Fig. 2 A). The expression of osterix, ALP, and Ocn was increased in Panx3-overexpressing cells compared with control cells transfected with vector pEF1, whereas the Runx2 expression level was unaffected in both cell types (Fig. 2 A). When endogenous Panx3 expression was inhibited by shPanx3 RNA transfection (Fig. S1, A and B), the induction levels of the osterix, ALP, and Ocn, but not of Runx2, were reduced (Fig. 2 B). Panx3 overexpression also promoted ALP activity and mineralization, whereas suppression of endogenous Panx3 by shPanx3 inhibited these processes (Fig. 2, C and D). We observed similar results in primary calvarial cells (Fig. S2, A, B, and C). Collectively, these findings indicated that Panx3 promotes osteoblast differentiation processes.

during osteoblast differentiation in both cell types. Runx2, osterix, ALP, and Ocn are osteoblast differentiation marker genes. Nat1 was used as a control. (C, a) Cellular localization of endogenous Panx3 in undifferentiated (a–c) and differentiated C2C12 cells (d–f) after 4 d of culture with BMP2. Panx3 (red) was localized in the plasma membrane, cell–cell junctions, and ER membranes in differentiated cells. Calnexin was used as an ER marker. (b) Measurements show a percentage of colocalization between Panx3 with calnexin (top), and calnexin with Panx3 (bottom). *, $P < 0.05$. Error bars represent the mean ± SD; $n = 12$.

Published June 20, 2011

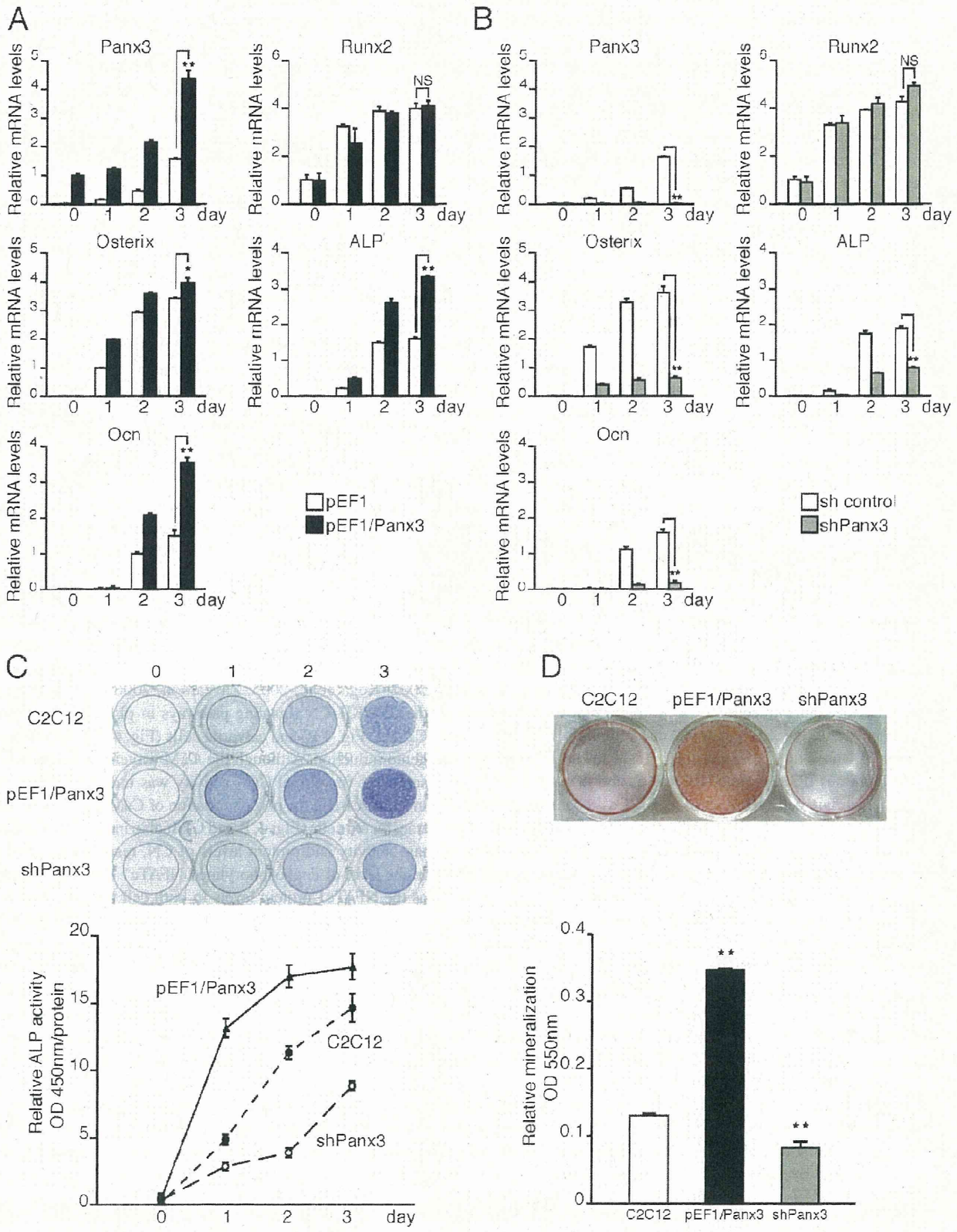

Figure 2. **Panx3 promotes osteoblast differentiation.** C2C12 cells were transiently transfected with a control pEF1 vector, pEF1/Panx3, a control sh vector, or a Panx3 shRNA vector, and these cells were cultured with BMP2 for various durations, as indicated. Total RNA was extracted each day for 4 d and mRNA levels were analyzed by quantitative RT-PCR. (A) Panx3 overexpression promoted the expression of osteoblast marker genes for osterix, ALP, and Ocn, except that the expression of Runx2 remained the same. (B) shPanx3 suppressed the induction of these genes, except for Runx2. (C) Panx3

Published June 20, 2011

Panx3 promotes metatarsal bone growth

Because Panx3 was expressed in the perichondrium/periosteum and osteoblasts, we analyzed Panx3 functions further with respect to ex vivo growth of the metatarsus. Metatarsal bones from newborn mice were cultured and infected with Panx3 expression adenovirus (AdPanx3). AdPanx3 promoted growth in the length and width of both cartilage and bone in metatarsus after 3 d in culture compared with the growth in the control adenovirus-infected metatarsus, as shown in videos and histology sections (Fig. 3 A, a; Fig. 3 B, a and b; and Videos 1 and 2). AdPanx3 infection increased not only the expression of Panx3, but also the expression of the osteoblast marker genes osterix, ALP, and Ocn (Fig. 3 C). To inhibit endogenous Panx3 activity, we used an inhibitory Panx3 peptide from the extracellular domain of Panx3, which blocked hemichannel activity and the release of ATP release (see Fig. 6), as described previously (Iwamoto et al., 2010). Addition of the Panx3 peptide to a metatarsus culture inhibited the growth in length and width compared with the growth without the peptide or growth in a culture with a control scrambled peptide (Figs. 3 A, b; Fig. 3 B, a and b; and Videos 3 and 4). The Panx3 peptide inhibited the expression of osteoblast marker genes (Fig. 3 C), which indicates that Panx3 regulates growth plate expansion.

Panx3 functions as an ER Ca^{2+} channel

Because the intracellular Ca^{2+} level ($[Ca2^{+}]_i$) plays an important role in osteoblast differentiation (Zayzafoon et al., 2005; Seo et al., 2009), we examined whether intracellular Ca^{2+} signaling is involved in Panx3-promoted osteoblast differentiation. The ER serves as the main intracellular Ca^{2+} storage compartment. In the ER membrane, the sarco/endoplasmic reticulum Ca^{2+}-ATPase (SERCA) takes up Ca^{2+} from the cytosol to the ER, whereas the ubiquitous IP3 receptors (IP3R1, -2, and -3), as well as the RyRs in certain cell types, serve as ER Ca^{2+} channels for Ca^{2+} release from the ER (Keller and Grover, 2000; Fill and Copello, 2002; Futatsugi et al., 2005). Extracellular ATP can bind to purinergic receptors (P2Rs) and subsequently activate downstream intracellular signaling cascades. These signaling pathways are known to promote IP3 production, thereby activating IP3R ER Ca^{2+} channels and increasing $[Ca^{2+}]_i$ (Solini et al., 2008). In C2C12 cells, all IP3Rs are expressed, with IP3R3 showing the highest expression level (Powell et al., 2001), whereas RyRs are not expressed (Fig. S1 C; Biswas et al., 1999). No significant change was observed in the expression levels of IP3Rs during osteogenic differentiation of C2C12 (Fig. S1 C). Because Panx3 was induced during differentiation of C2C12 and calvarial cells and was localized in the ER, Panx3 may function as an ER Ca^{2+} channel, thereby increasing $[Ca^{2+}]_i$ and subsequently promoting osteoblast differentiation. To explore Panx3 Ca^{2+} ER channel activity, Panx3 overexpressing C2C12 and calvarial cells were loaded with a UV-excitable intracellular Ca^{2+} indicator, Fura-2 AM, in Ca^{2+}-free media. The cells were then stimulated by ATP, and increases in the $[Ca^{2+}]_i$ level were measured over a time course and compared with $[Ca^{2+}]_i$ levels in control cells lacking Panx3 (Fig. 4 A, a and b). $[Ca^{2+}]_i$ was approximately twofold higher in Panx3-overexpressing C2C12 and calvarial cells than in control cells. This suggests that Panx3 may act as an ER Ca^{2+} channel.

To measure steady-state $[Ca^{2+}]_i$ levels during differentiation, C2C12 cells were cultured with BMP2, and $[Ca^{2+}]_i$ was analyzed without ATP stimulation (Fig. 4 A, c). The level of $[Ca^{2+}]_i$ in undifferentiated C2C12 cells was ~100 nM, a concentration typically observed in cells at rest. At 5 d after differentiation by BMP2, $[Ca^{2+}]_i$ was increased to ~180 nM, and this $[Ca^{2+}]_i$ increase was further enhanced to ~225 nM in Panx3-overexpressing C2C12 cells. Inhibition of differentiation by shPanx3 reduced $[Ca^{2+}]_i$. Collectively, these results suggest that Panx3 regulates $[Ca^{2+}]_i$. Similar $[Ca^{2+}]_i$ increases in calvarial cells were observed during osteogenic differentiation (Fig. S2 D).

Panx3 activates the CaM pathways for differentiation

Intracellular Ca^{2+} activates and affects many signaling pathways that modulate cell differentiation (Berridge et al., 2000a). Upon Ca^{2+} binding, CaM activates many downstream signaling molecules such as CaMKII and the phosphatase CN, and promotes osteoblast differentiation (Berridge et al., 2000b; Seo et al., 2009). NFATc1 is activated through dephosphorylation by CN and can promote expression of genes such as osterix, a key molecule involved in osteogenesis (Beals et al., 1997; Nakashima et al., 2002; Koga et al., 2005; Zayzafoon, 2006). We first examined the CaMKII–CN signaling pathways in pEF1/Panx3-transfected C2C12 (Fig. 4 B) and calvarial cells (Fig. 4 C) after short osteogenic induction. Although the CaM protein level remained the same, we found that CaM activity was induced, which resulted in an increase in the phosphorylation of CaMKII in pEF1/Panx3-transfected cells (Fig. 4, B and C). It also increased the phosphatase activity and protein levels of CN, resulting in an increase in the level of dephosphorylated NFATc1 (active form) as well as the NFATc1 protein levels in both cell types compared with control cells. The increase in NFATc1 protein levels is likely caused by the enhanced NFATc1 transcription levels in the CaMKII–c-fos pathway (Koga et al., 2005; Zayzafoon et al., 2005). In a subsequent experiment involving the inhibition of endogenous Panx3 expression, shPanx3- and shControl-transfected cells were cultured under induction conditions for 1 d to induce endogenous Panx3, and the activation of these factors was measured. Inhibition with shPanx3 reduced the phosphorylation levels of CaMKII and increased inactive phosphorylated NFATc1 levels in C2C12 cells and to a lesser extent in calvarial cells (Fig. 4, B and C). The effects of Panx3 on the CaM pathways were less prominent in calvarial cells than in C2C12 cells, likely because of differences in their transfection efficiency. pEF1/Paxn3 and

overexpression promoted ALP activity, whereas shPanx3 inhibited it. Representative ALP staining (top) and its quantitative data (bottom). C2C12 cells and pEF1/Panx3- and shPanx3-transfected C2C12 cells were cultured with BMP2 for 3 d. (D) Representative Alizarin red S staining (top) and its quantitative data (bottom) of C2C12 and pEF1/panx3- and shPanx3-transfected C2C12 cells cultured with BMP2 for 15 d. **, $P < 0.01$. Error bars represent the mean ± SD; $n = 3$.

Published June 20, 2011

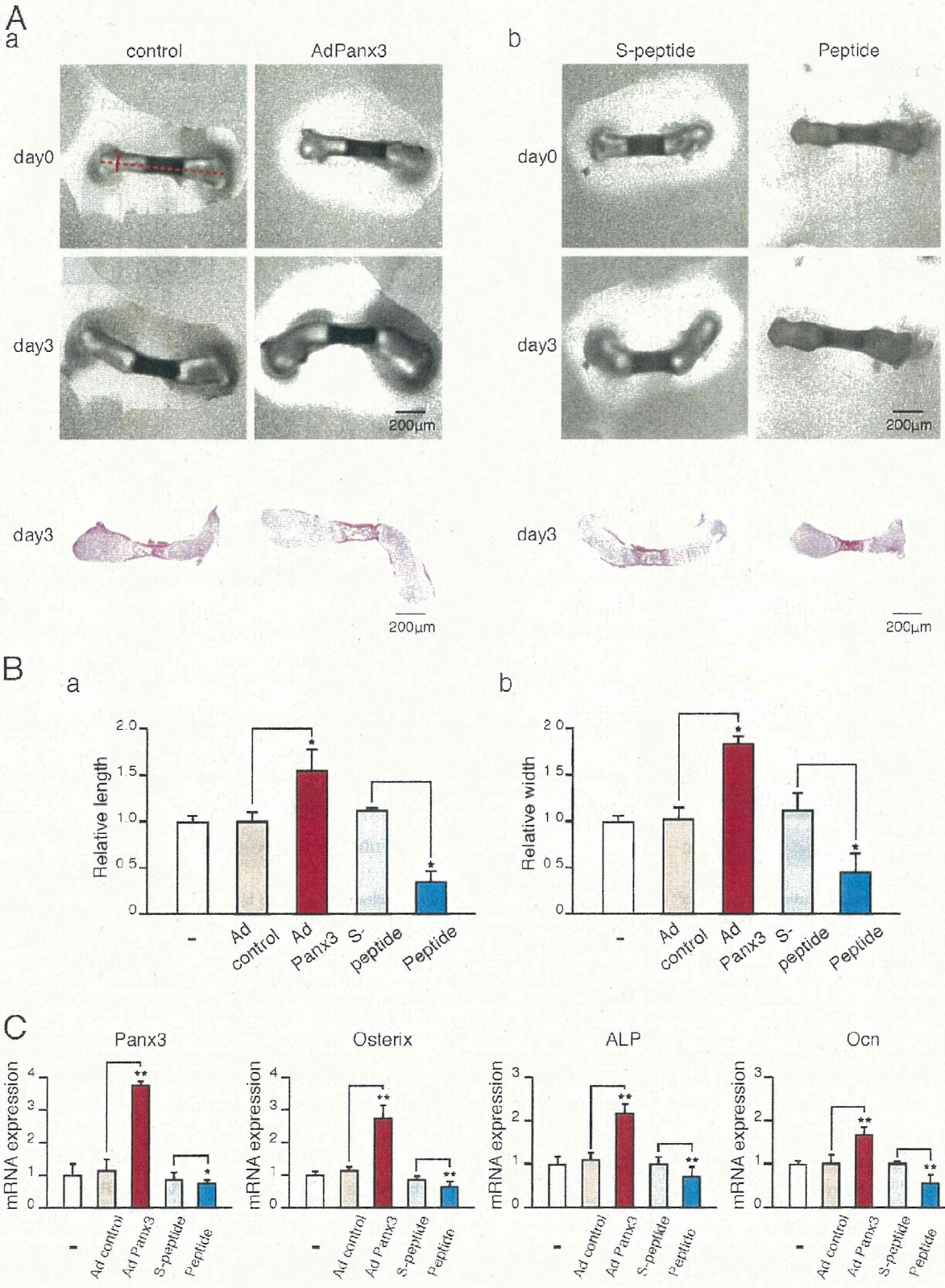

Figure 3. **Panx3 promotes the growth of metatarsus ex vivo.** (A) Live images of ex vivo metatarsal growth (top) and histology (bottom). (a) Newborn mouse metatarsal bones were cultured and infected with Panx3 adenovirus (AdPanx3) or control adenovirus. (b) Metatarsus cultures were incubated with the Panx3 peptide for 3 d. Metatarsal bone growth was measured by real-time imaging. AdPanx3 promoted metatarsal bone growth (a), whereas the Panx3 peptide inhibited it (b). (B) Relative change in metatarsal length (Ba) or width (Bb) after 3 d in culture compared with day 0. The bone length was

Published June 20, 2011

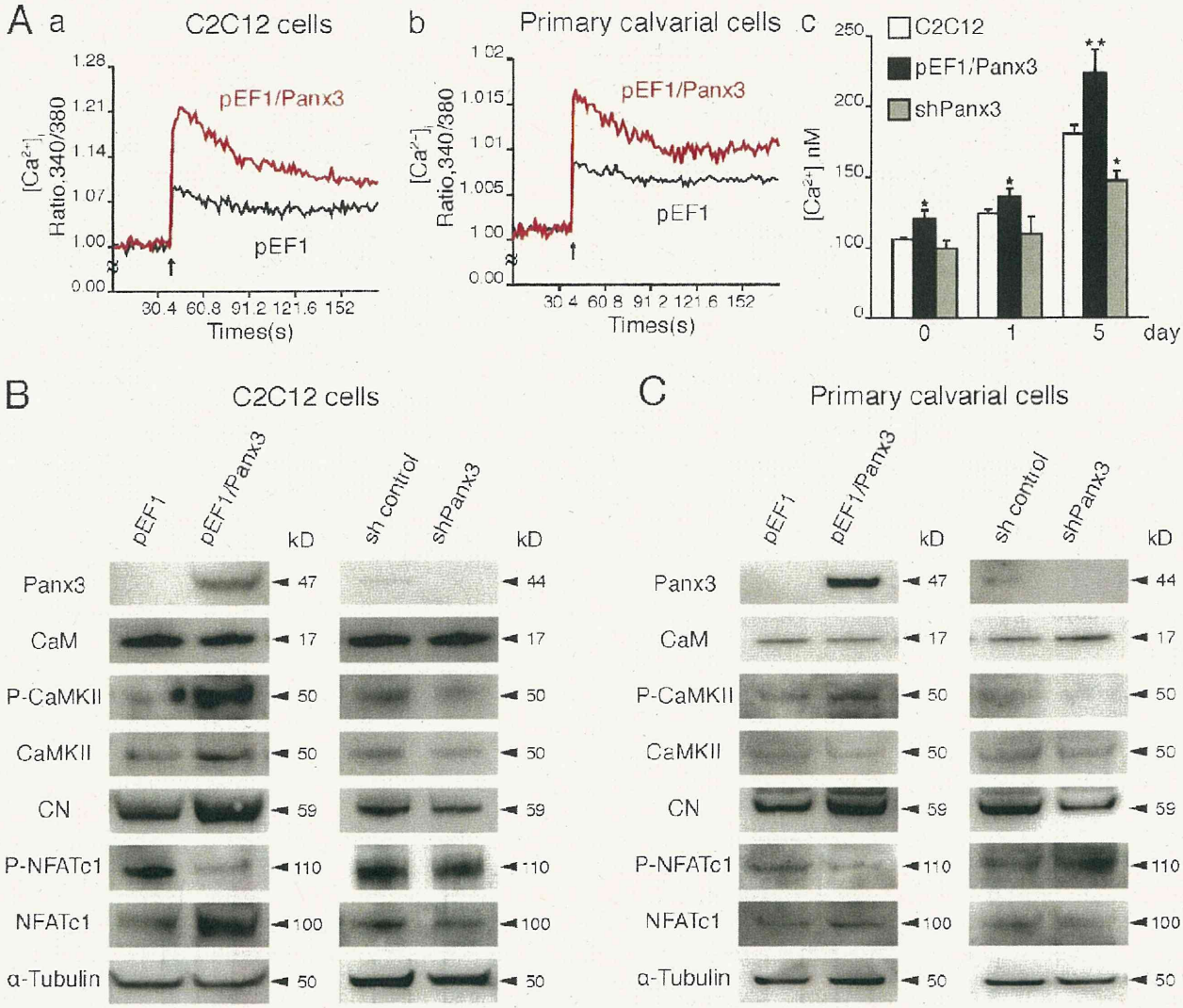

Figure 4. **Panx3 functions as an ER Ca^{2+} channel, and activates the CaM and Akt pathways.** (A, a and b) Panx3 ER Ca^{2+} channel. C2C12 cells stably transfected with pEF1 (black) or pEF1/Panx3 (red) expression vectors were analyzed for ATP-stimulated $[Ca^{2+}]_i$ in a time course (A, a). Primary calvarial cells were transiently transfected with pEF1 (black) or pEF1/Panx3 (red) expression vectors (A, b). The data shown are representative of at least four different experiments. (A, c) $[Ca^{2+}]_i$ levels during differentiation of C2C12 cells. Untransfected and stably transfected cells with pEF1/Panx3 or shPanx3 vectors were cultured with BMP2 at the indicated days. $[Ca^{2+}]_i$ levels in pEF1/Panx3-transfected cells were much higher than in C2C12 cells, whereas those in shPanx3 cells were lower. *, $P < 0.05$; **, $P < 0.01$. Error bars represent the mean ± SD, $n = 3$. (B and C) Panx3 activates the CaM/NFATc1 signaling pathways. C2C12 cells or primary calvarial cells were stably and transiently transfected with pEF1 and pEF1/Panx3 vectors, respectively, then incubated for 1 h with BMP2, and the levels of the signal molecules were analyzed by Western blotting. For shPanx3 inhibition experiments, stably transfected C2C12 cells or transiently transfected primary calvarial cells with sh control and shPanx3 RNA were cultured for 1 d in the presence of BMP2.

shPanx3 were transiently transfected into calvarial cells, whereas they were stably transfected into C2C12 cells.

Activation mechanism of Panx3 ER Ca^{2+} channel

Next, we determined whether any differences existed between the activation mechanisms of the Panx3 and IP3R ER Ca^{2+} channels by using inhibitors of the IP3R function (Vanden Abeele et al., 2006). In control undifferentiated C2C12 cells, 2-APB, an inhibitor of IP3-induced Ca^{2+} release (Maruyama et al., 1997), completely blocked Ca^{2+} release from the IP3R channel in control cells (Fig. 5 A, a). In Panx3-overexpressing undifferentiated C2C12 cells, 2-APB treatment resulted in a reduction in the $[Ca^{2+}]_i$ levels, which closely corresponded to the

measured from edge to edge (A, a, broken red line). The width was measured from side to side (A, a, red line). AdPanx3 promoted the growth of both length and width, whereas Panx3 peptide inhibited both. (C) Quantitative RT-PCR. Metatarsus cultures were incubated for 3 d with AdPanx3 or the Panx3 peptide. AdPanx3 promoted the expression of osteoblast marker genes, osterix, ALP, and Ocn. The Panx3 peptide inhibited this marker gene expression. *, $P < 0.05$; **, $P < 0.01$. Error bars represent the mean ± SD; $n = 3$.

Published June 20, 2011

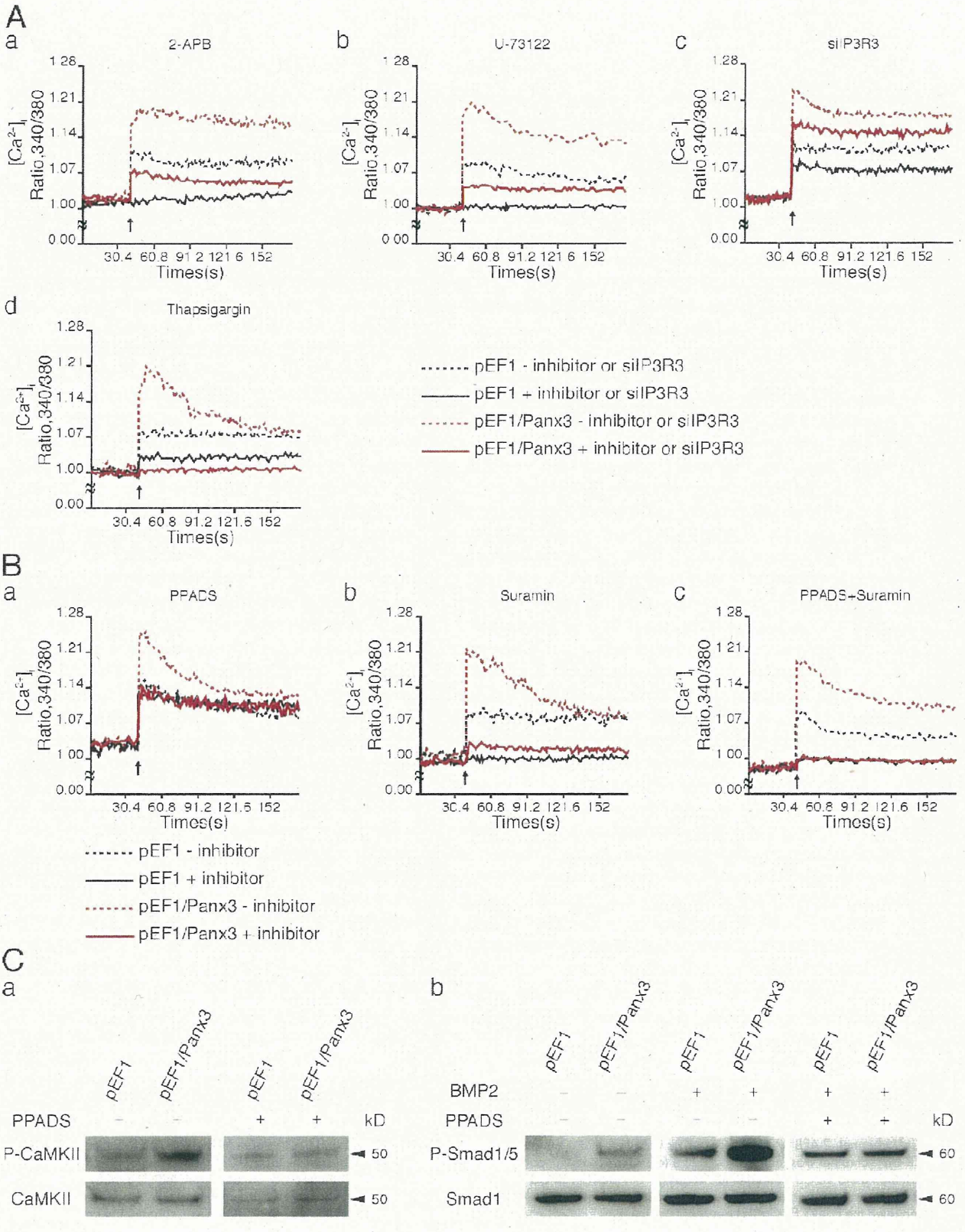

Figure 5. **Panx3 ER Ca^{2+} channel activation and its downstream signaling.** C2C12 cells stably transfected with pEF1 or pEF1/Panx3 expression vectors were analyzed for ATP-stimulated $[Ca^{2+}]_i$. Inhibitors were added to the cell culture for 30 min before ATP stimulation. In inhibition to endogenous IP3R3 expression, $[Ca^{2+}]_i$ was analyzed after 3 d of transfection of C2C12 cells with siRNA for IP3R3. (A) Panx3 ER Ca^{2+} channel independent of the IP3R ER

Published June 20, 2011

$[Ca^{2+}]_i$ levels in control cells (Fig. 5 A, a). This indicates that 2-APB inhibited the IP3R ER Ca^{2+} channel, but not the Panx3 ER Ca^{2+} channel. In control cells, U-73122, a selective inhibitor of PLC, which catalyzes DAG and IP3 synthesis (Bleasdale et al., 1990), completely blocked the IP3R Ca^{2+} channel (Fig. 5 A, b); however, it only partially inhibited the Panx3 ER Ca^{2+} channel (Fig. 5 A, b). Inhibition of endogenous IP3R3 expression by siRNA reduced the IP3R Ca^{2+} channel but not the Panx3 ER Ca^{2+} channel (Fig. 5 A, c). Thapsigargin, a highly selective inhibitor of the SERCA ER Ca^{2+} pumps responsible for loading Ca^{2+} stores (Inesi and Sagara, 1992), partially inhibited IP3R-mediated Ca^{2+} release from the ER in control cells (Fig. 5 A, d), whereas it completely blocked Ca^{2+} release from the ER in Panx3-overexpressing cells (Fig. 5 A, c). This suggests that the Panx3 ER Ca^{2+} channel continuously released Ca^{2+} from the ER after thapsigargin treatment. Therefore, the activation mechanism for the Panx3 ER Ca^{2+} channel appears to be different from that of the IP3R.

Because Panx3 and IP3R ER Ca^{2+} channels are both activated by external ATP, we tested the differences in ATP receptors involved in the activation of these channels. ATP receptors (purinergic receptors, P2Rs) consist of two subtypes, the ligand-gated cation channels (P2Xs) and the G protein–coupled receptors (P2Ys; Burnstock and Knight, 2004). During osteoblast differentiation, a series of P2X and P2Y subtypes are expressed (Hoebertz et al., 2000; Orriss et al., 2006; Panupinthu et al., 2008). To examine whether specific subtypes of P2Rs are required for the activation of the Panx3 ER Ca^{2+} channel, the P2R antagonists pyridoxal-phosphate-6-azophenyl-2′,4′-disulfonate (PPADS) and suramin were tested for their effects on ATP-stimulated changes in $[Ca^{2+}]_i$ in Panx3-overexpressing and control cells (Fig. 5 B). PPADS inhibited Panx3 ER Ca^{2+} channel activity in Panx3-overexpressing C2C12 cells (Fig. 5 B, a), whereas it did not inhibit the IP3R Ca^{2+} channel in control cells (Fig. 5 B, a). Suramin completely inhibited the IP3R Ca^{2+} channel in control cells (Fig. 5 B, b), and partially inhibited the Panx3 ER channel in Panx3-overexpressing cells (Fig. 5 B, b). A combination of PPADS and suramin completely inhibited both Panx3 and IP3R ER channels (Fig. 5 B, c). These results indicated that the Panx3 ER Ca^{2+} channel is activated through PPADS-sensitive P2Rs that are distinct from the IP3R channel.

Because PPADS specifically inhibited the Panx3 ER Ca^{2+} channel, we tested whether it would also inhibit Panx3-mediated CaM activation. For these experiments, we treated control and Panx3 overexpressing C2C12 cells with BMP-2 for 1 h and then analyzed the phosphorylation of CaMKII and Smad1/5, both of which are targets of CaM (Fig. 5 C; Wicks et al., 2000; Pardali et al., 2005). PPADS inhibited phosphorylation of CaMKII induced by Panx3 overexpression (Fig. 5 C, a). Without BMP2 treatment, Panx3 overexpression resulted in activation of Smad1/5 (Fig. 5 C, b, left). BMP2 induced phosphorylation of Smad1/5 in control cells, and Panx3 overexpression further increased phosphorylation levels of Smad1/5 (Fig. 5 C, b, middle), whereas this stimulation was blocked by PPADS (Fig. 5 C, b, right). These results suggest that the activation of specific P2Rs may be involved in Panx3-mediated signaling for osteoblast differentiation through CaMKII and Smad1/5 pathways.

Panx3 activates the Akt pathway

In addition to P2R-mediated activation of the PLC–PIP2–IP3–IP3R pathway, P2Rs also activate PI3K signaling. Because Akt downstream from PI3K is crucial for osteoblast differentiation (Fujita et al., 2004; Mukherjee and Rotwein, 2009), we explored the involvement of Akt in Panx3-promoted osteoblast differentiation. We found that Panx3 overexpression increased phosphorylation of Akt and Akt-downstream MDM2, and promoted the degradation of p53 in both C2C12 and calvarial cells (Fig. 6 A, a and b). p53 is a negative regulator of osteogenesis (Lengner et al., 2006) and inhibits Runx2 and osterix expression (Lian et al., 2006). Akt-mediated MDM2 phosphorylation leads to p53 ubiquitination (Ogawara et al., 2002). Our results indicate that Panx3 expression activates Akt and promotes p53 degradation through MDM2 activation.

An Akt inhibitor reduced the expression of osterix mRNA in control and pEF1/Panx3-transfected C2C12 cells. The dominant-negative Akt vector (Akt DN) also inhibited osterix expression, whereas the activated Akt vector increased the expression (Fig. 6 B, a). Similar results were found for ALP expression (Fig. 6 B, b). These results suggest that Panx3 promotes osteoblast differentiation in part through the Akt pathway.

Akt activates the Panx3 ER Ca^{2+} channel

We next examined the involvement of Akt in the activation of a Panx3 ER Ca^{2+} channel. We found that the Akt inhibitor abolished ATP-stimulated Panx3 ER Ca^{2+} channel activity in Panx3-overexpressing C2C12 cells (Fig. 7 A, a). The remaining Ca^{2+} released from the ER was likely through the IP3R ER Ca^{2+} channel, which showed an activity level similar to that in control cells. The Akt inhibitor did not inhibit the IP3R ER Ca^{2+} channel in control cells. Akt DN also inhibited the ATP-stimulated Panx3 ER Ca^{2+} release, but not IP3R ER Ca^{2+} release (Fig. 7 A, b). In contrast, activated constitutively active Akt (Akt CA) increased the activity of the Panx3 ER Ca^{2+} channel, but not the activity of the IP3R ER Ca^{2+} channel (Fig. 7 A, c). In control cells, neither

Ca^{2+} channel. 2-APB (IP3R inhibitor; a) or U-73122 (IP3 synthesis inhibitor; b) completely inhibited Ca^{2+} release from the IP3R ER Ca^{2+} channel. The Panx3 ER Ca^{2+} channel was inhibited by 2-APB (a), whereas it was partially inhibited by U-73122 (b). siRNA for IP3R3 inhibited the IP3R3 ER Ca^{2+} channel, but not the Panx3 ER Ca^{2+} channel (c). Thapsigargin (SERCA ER Ca^{2+} pump inhibitor) completely inhibited Ca^{2+} release from the ER in pEF1/Panx3-transfected cells, whereas it partially inhibited it in pEF1-transfected cells (d). The data shown are representative of at least three different experiments. (B) PPADS inhibited the Panx3 ER Ca^{2+} channel but not the IP3R ER Ca^{2+} channel (a). Suramin completely inhibited the IP3R ER Ca^{2+} channel but partially inhibited the Panx3 ER Ca^{2+} channel (b). A combination of PPADS and suramin blocked both ER Ca^{2+} channels (c). Arrows indicate the time of ATP addition. The data shown are representative of at least three different experiments. (C) PPADS inhibition of CaM downstream signaling. Stably transfected C2C12 cells with pEF1 and pEF1/Panx3 vectors were incubated for 1 h with BMP2, with or without PPADS, and levels of phosphorylation of CaMKII (a) and Smad1/5 (b) phosphorylation were analyzed by Western blotting. The left panel in b indicates Smad1/5 phosphorylation levels in cells without BMP2 and PPADS. In the middle and right panels of b, cells were induced by BMP2.

Published June 20, 2011

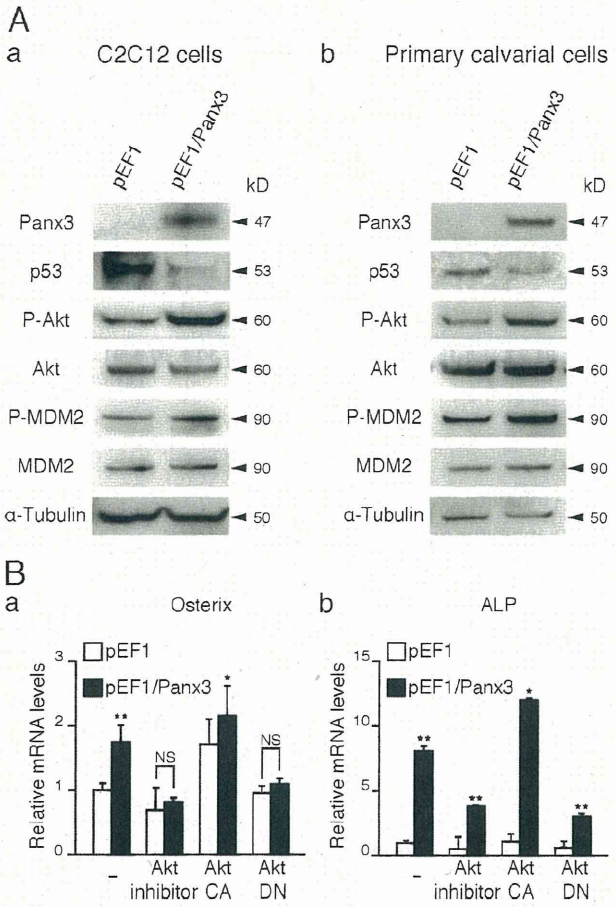

Figure 6. **Panx3 activates the Akt pathway.** (A, a and b) Panx3 activates Akt signaling. Stably transfected C2C12 cells or transiently transfected primary calvarial cells with pEF1 and pEF1/Panx3 vectors were incubated for 1 h with BMP2, and levels of signal molecules were analyzed by Western blotting. Panx3 expression increased phosphorylation of Akt and MDM2 and promoted p53 degradation. (B) Akt inhibition reduced Panx3-promoted expression of osterix (a) and ALP expression (b). The transfected cells were cultured with BMP2 for 3 d, and the expression of osterix and ALP was analyzed by real-time PCR. The Akt inhibitor and Akt DN inhibited the expression of Panx3-mediated induction of these genes, whereas Akt CA increased the expression levels in control and Panx3-overexpressing cells. *, $P < 0.05$; **, $P < 0.01$. Error bars indicate the mean ± SD; $n = 3$.

Akt vector affected the IP3R ER Ca^{2+} channel (Fig. 7 A, b and c). LY294002, an inhibitor of PI3K, inhibited both Panx3 and IP3R ER channels (Fig. 7 A, d). The reason for this was that PI3K activates Akt as well as the IP3 synthesis pathway (Carpenter and Cantley, 1996). These results suggest that ATP-stimulated activation of the Panx3 ER Ca^{2+} channel is mediated through a PI3K–Akt activation that is distinct from the IP3-dependent activation of IP3R ER Ca^{2+} channels.

To further confirm the Akt-mediated activation of the Panx3 ER Ca^{2+} channel, the $[Ca^{2+}]_i$ concentration was measured without ATP stimulation (Fig. 7 B). The steady-state $[Ca^{2+}]_i$ concentration in Panx3-overexpressing C2C12 cells was ~140 nM, which was higher than that of control cells (90 nM). The activated Akt enhanced the $[Ca^{2+}]_i$ concentration in Panx3-overexpressing C2C12 cells by about twofold (280 nM) compared with that in cells without the Akt vector. Akt DN reduced the steady-state $[Ca^{2+}]_i$ concentration in Panx3-overexpressing C2C12 cells to a level similar to that seen in the control cells. These results indicated that the Panx3 ER Ca^{2+} channel is regulated by Akt signaling, and that its mechanism is independent of IP3R activity.

We further examined whether Akt-mediated Panx3 ER Ca^{2+} channel activation regulates the CaM–CaMKII–NFATc1 signaling pathways (Fig. 7 C). Panx3-overexpressing C2C12 cells were transfected with the Akt CA or Akt DN vector and were treated with BMP2 for 1 h. Western blotting analysis showed that Akt CA increased phosphorylation of CaMKII (P-CaMKII) and activation of NFATc1 (reduced P-NFATc1), whereas Akt DN inhibited CaMKII and NFATc1 activation (Fig. 7 C). These results support the notion that the Akt signaling pathway regulates the Panx3 ER Ca^{2+} channel.

Panx3 releases intracellular ATP through its hemichannel activity

The activation of P2Rs may be caused in part by binding of ATP released from cells through Panx3 hemichannel activity. To test this possibility, we first analyzed the intracellular ATP levels in control and Panx3-overexpressing C2C12 cells by fluorescence imaging using confocal microscopy (Fig. 8 A, a). The cells containing caged luciferin were illuminated by a flash of two-photon light, which photolyzed the caged luciferin, allowing the uncaged luciferin to bind to intracellular ATP and resulting in an increase in fluorescence emissions. The fluorescence intensity at 5 and 15 s after photolysis was much higher (red) in control C2C12 cells than in Panx3-overexpressing cells, which suggests that Panx3 expression reduced intracellular ATP levels. To analyze ATP release, control and Panx3-overexpressing C2C12 and calvarial cells were incubated in the presence of luciferin for 2 min, and the fluorescence intensity was measured (Fig. 8 A, b and c). The extracellular ATP level was approximately twofold higher in Panx3-expressing cells than in control cells. Similar results were obtained when the cells were treated with KGlu to depolarize the cell membrane, except that the level of ATP release was much higher. Addition of anti-Panx3 antibody, but not IgG, to the cell culture assay inhibited Panx3-mediated ATP release (Fig. 8 B, a). To test whether this inhibition was specific to Panx3, we used the inhibitory Panx3 peptide from the extracellular domain of Panx3, which had been used as an antigen for the Panx3 antibody (Iwamoto et al., 2010). The peptide, but not a scrambled peptide, blocked the inhibitory activity of the antibody for the ATP release in a dose-dependent manner (Fig. 8 B, a). In addition, the Panx3 peptide alone showed inhibitory activity for the ATP release, as described previously in chondrogenic ATDC5 cells (Iwamoto et al., 2010). Under differentiation conditions, suppression of endogenous Panx3 by shRNA inhibited ATP release in C2C12 cells (Fig. 8 B, b). These results indicated that Panx3 caused the release of intracellular ATP into the extracellular space though the hemichannel.

To test the effects of the Panx3 hemichannel on osteoblast differentiation, control and Panx3-overexpressing C2C12 cells were induced to differentiate by a 2-d treatment with BMP2, in the presence or absence of the anti-Panx3 antibody, and mRNA levels for osterix and ALP were analyzed (Fig. 8 C). The Panx3 antibody inhibited the induction of osterix and ALP expression

Published June 20, 2011

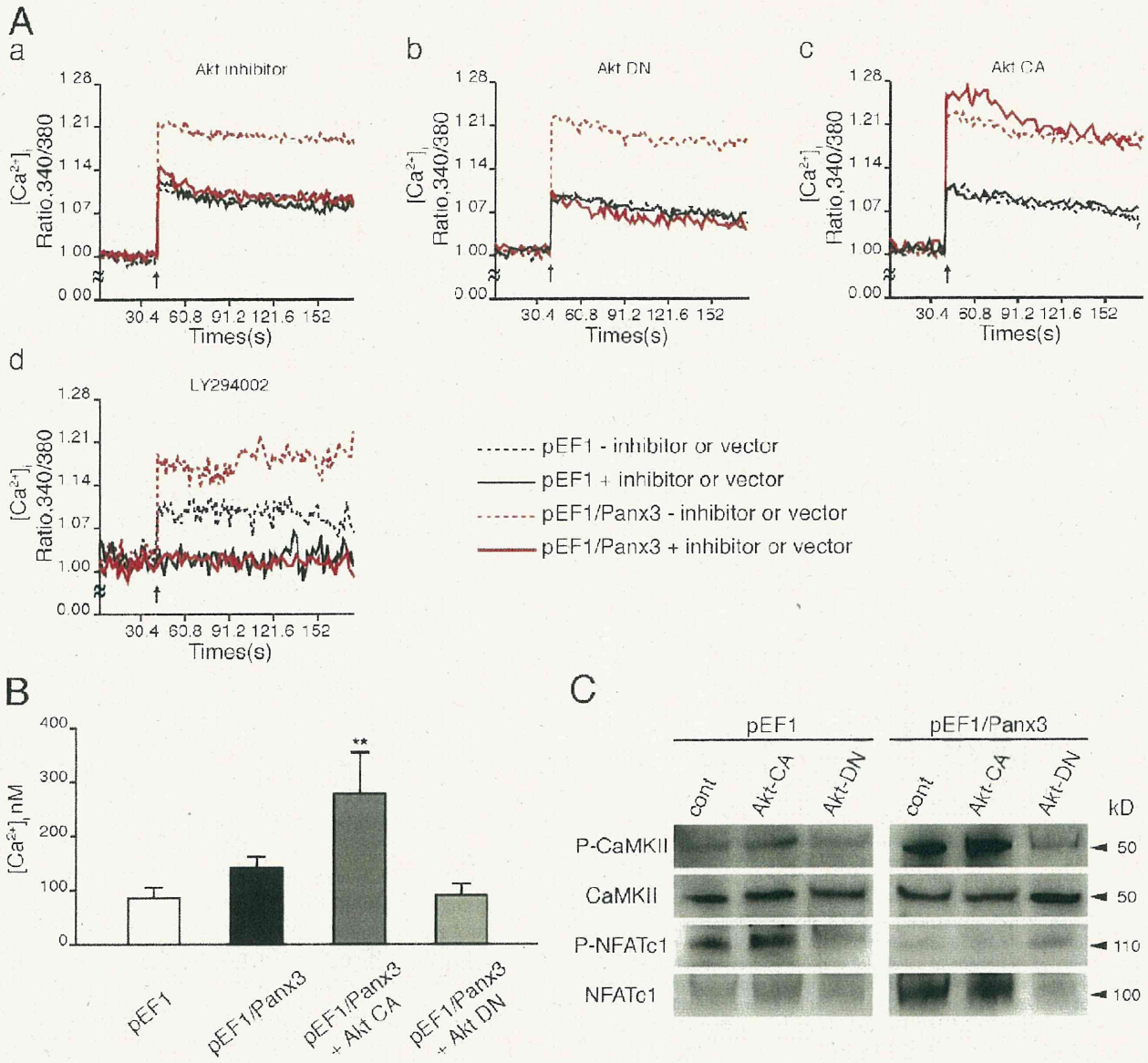

Figure 7. **Activation of Panx3 ER Ca^{2+} channel by PI3K–Akt signaling.** (A) pEF1- or pEF1/Panx3-transfected C2C12 cells were incubated with the Akt inhibitor (a), or transfected with the dominant-negative Akt (Akt DN; b), the activated Akt (Akt CA) vector (c), or LY294002 (PI3K inhibitor; d). $[Ca^{2+}]_i$ was measured by the fluorescence intensity ratio of Fura-2 (F_{340nm}/F_{380nm}) in each condition. The Akt inhibitor blocked the Panx3 ER Ca^{2+} channel (a). Akt DN inhibited the Panx3 ER Ca^{2+} channel, not the IP3R ER channel (b). Akt CA promoted the Panx3 ER Ca^{2+} channel, not the IP3R ER channel (c). LY294002 inhibited Ca^{2+} release from both Panx3 and IP3R ER Ca^{2+} channels (d). Arrows indicate the time of ATP addition. The data shown are representative of at least three different experiments. (B) The $[Ca^{2+}]_i$ level was increased by Akt activation. The basal levels of $[Ca^{2+}]_i$ in Panx3-overexpressing C2C12 (pEF1/Panx3) cells are higher than in control vector–transfected (pEF1) cells. Akt CA increased $[Ca^{2+}]_i$ in pEF1/Panx3 cells, whereas Akt DN reduced $[Ca^{2+}]_i$ to similar levels in control cells. (C) The transfected cells were induced by BMP2 for 1 h, and phosphorylation of CaMKII and NFATc1 was analyzed by Western blotting. Akt increased CaMKII and NFATc1 phosphorylation levels in control cells, and Panx3 overexpression further enhanced its activation. Akt DN inhibited these activations to the levels in control cells. *, $P < 0.05$; **, $P < 0.01$. Error bars indicate the mean ± SD; $n = 3$.

in both control and Panx3-overexpressing cells. Because the antibody and peptide blocked the Panx3 hemichannel activity, these results suggest that the Panx3 hemichannel plays a critical role in osteoblast differentiation.

Panx3 gap junction function during osteoblast differentiation

An increase in $[Ca^{2+}]_i$ in one cell can be transmitted to neighboring cells, resulting in Ca^{2+} waves that spread within cell networks. This Ca^{2+} wave propagation is mediated by gap junctions and promotes cell–cell communication for cellular processes and differentiation (Barbe et al., 2006). Therefore, we examined Panx3 gap junction activity in C2C12 cells and its effect on osteoblast differentiation (Fig. 9). First, Ca^{2+} wave propagation in Panx3-overexpressing C2C12 cells was analyzed and compared with that in control cells. The cells were loaded with a photosensitive caged form of Ca^{2+} and Ca^{2+}-sensitive Fluo-4. While performing live-cell Ca^{2+} imaging, a